

SPACE NAVIGATION APPLICATIONS

Peter M. Kachmar
C.S. Draper Laboratory, Cambridge, MA

Lincoln Wood
Jet Propulsion Laboratory, California Institute of Technology, Pasadena, CA

ABSTRACT

Over the past twenty-five years, we have witnessed the extraordinary achievements of both robotic and manned space missions. A key element in the success of these missions has been the development of the navigation systems that have enabled the determination of the current and predicted spacecraft position and velocity to the accuracies required to meet mission objectives. This paper presents an overview of space navigation systems, navigation techniques and capabilities for robotic and manned mission applications for the past twenty-five years.

Robotic navigation systems data types, information content, and navigation data processing techniques are reviewed. Application of these systems to planetary missions are discussed, including Mariner 9 and 10, Viking, Voyager, Mission to Halley, Comet, Magellan and Galileo.

For manned space navigation systems, the role of on-board and ground navigation capabilities is presented. Key technology developments that enabled the development of on-board systems are discussed. Ground and on-board navigation data types and their information content, data processing techniques and system operations are reviewed. Application of these ground and on-board systems to Apollo, Skylab, Apollo/Soyuz, Space Shuttle and Space Station are presented. Finally, a look at the future of space navigation is presented. The application and extension of current navigation concepts and of new navigation enhancing technologies to the future requirements of robotic and manned space navigation system are discussed.

SECTION 1. INTRODUCTION

Over the past twenty-five years, we have witnessed the extraordinary achievements of both robotic and manned space missions. These achievements have marked the beginnings of

mankind's exploration of space and of the use of space' based capabilities to provide knowledge of and improvement in the quality of life on our home planet.

Robotic mission encounters with most of the planets of our solar system (such as the Voyager Missions conceptually shown in Figure 1), the close up viewing and scientific observations of these planets, and the landing of robotic spacecraft on the moon and on Mars have provided a wealth of scientific information and a view of our solar system previously imaginable only to science fiction writers and their readers.

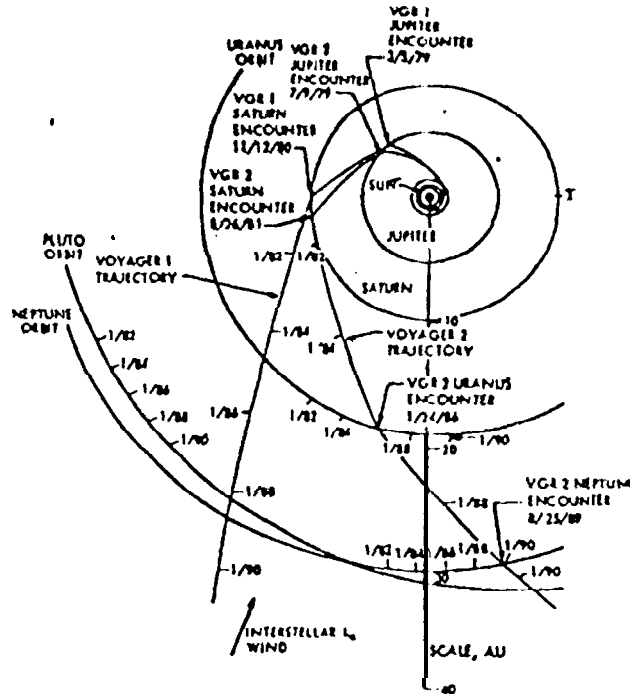


Figure 1, Planetary Robotic Missions - Voyager

Manned space missions have shown us the incredible ability, creativity and resourcefulness of men and women in living in the space environment, in performing scientific experiments and earth and lunar observation, in repairing spacecraft and in exploring the surface of the moon. From the images shown by these astronauts and cosmonauts and their words in describing their missions, experiments and observations, mankind has been provided a perspective that has inextricably transformed our understanding and view of the earth and our relationship to it. The Apollo lunar landing program, profiled in Figure 2, provided the first view of the earth in its entirety, marking the beginning of our view of the majesty and complexity of the "big, blue, marble."

A key element in the success of these robotic and manned missions has been the development of space navigation systems. Both ground based and on board the spacecraft, these systems have enabled the determination of the spacecraft state (position and velocity) to the accuracies required for determining and achieving desired earth and planetary orbits, for traversing interplanetary distances, for precise landings on the surface of the earth, the moon and other planetary bodies, and for the successful execution and subsequent analysis of scientific experiments during these mission phases.

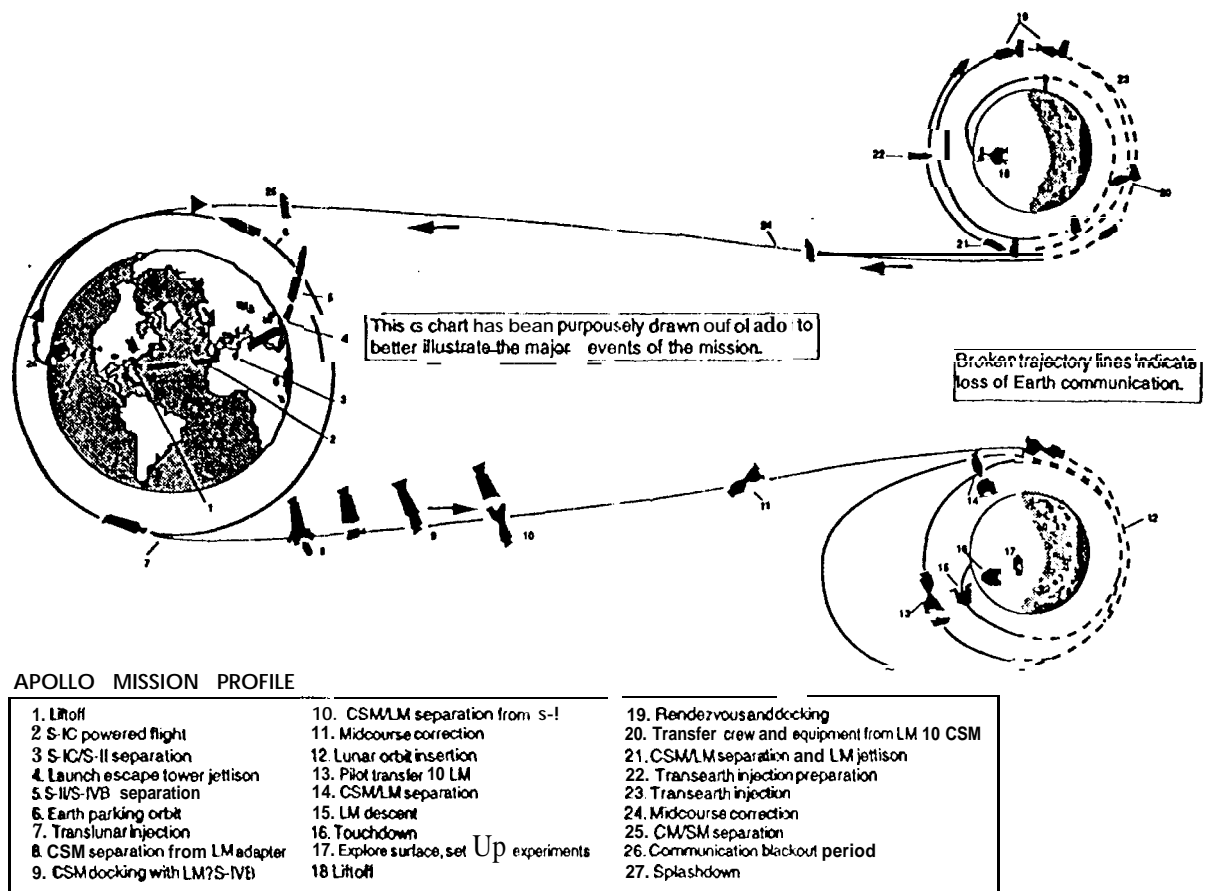


Figure 2. Apollo Manned Missions

This paper presents an overview of space navigation systems for robotic and manned mission applications for the past twenty-five years. Techniques and capabilities for both ground-based and on-board navigation system applications will be presented.

Section 2 discusses navigation objectives for robotic and manned mission applications. Similarities and differences between robotic and manned navigation applications will also be discussed.

Section 3 focuses on navigation systems for robotic mission applications. Navigation data types, information content, and navigation data processing techniques are reviewed. Planetary mission applications will be discussed with emphasis on the Voyager mission.

Section 4 focuses on manned space navigation systems. The key technologies that enable the development of on-board navigation systems for manned missions applications are discussed. These technologies span many technical disciplines and include: the enhanced processing capabilities of digital computers; the development of space qualified radio, optical, and inertial navigation aids which provide the measurements for these systems; and the development of recursive navigation algorithms for processing the measurements to determine the current spacecraft state. This section will review the role of on-board and ground navigation systems

and the operational interplay between them. Both ground and on-board navigation data types, their information content, data processing techniques, and system operations are presented. Applications of these systems to Apollo, Skylab, Apollo/Soyuz, Space Shuttle and the Space Station are discussed.

Finally, in Section 5, the application and extension of current navigation concepts and of new navigation enhancing technologies to the future requirements of robotic and manned space **navigation** systems, will be discussed. A possible lunar/Mars navigation infrastructure, and technology developments that will enhance current navigation system capabilities for automatic and autonomous vehicle operations **will also** be presented.

SECTION 2. SPACE NAVIGATION FOR **ROBOTIC** AND MANNED SPACE MISSIONS

Navigation systems, whether ground based or on board the spacecraft, must satisfy the basic objective of any navigation system: determine, through appropriate measurements or observations, the spacecraft position and velocity, and propagate this state forward, without benefit of measurements, with the accuracy required to accomplish mission objectives.

Robotic missions have both real-time and post-flight navigation requirements. The real-time requirements assure that the mission objectives can be met and that scientific and experimental data will be obtained within the operating constraints of the experiments and instruments **onboard** the spacecraft. The post-flight navigation requirements assure that the most accurate **state, determined** by post-flight processing of all relevant sensor information, is provided for the analysis of the scientific and experimental data obtained during the mission.

For manned space missions, the real-time navigation system requirements are of paramount importance. They determine, not only if the mission objectives can be met, but also the ultimate safety of the crew. Post-flight navigation requirements are used to determine the overall system performance so that the achievement of future mission objectives can be ensured and so that future missions can be made more demanding. In addition, the more accurate **post-flight navigation state** estimates can be used for improving the accuracy of experimental data.

2.1 Space Navigation System Objectives

Space navigation systems satisfy the basic objective with the following three requirements: 1. provide an estimate of the current and future (predicted) spacecraft **position and velocity** (referred to as the spacecraft state) to the accuracy required to achieve mission objectives; 2. provide these estimates within the **specified time** period required for their use (**latency** requirement); 3. provide these estimates with a specified degree of reliability (redundancy and failure mode requirement).

The current and predicted state estimates provided by the ground or on-board systems are used for targeting trajectory correction maneuvers to ensure the spacecraft state is within the required position and **velocity** envelope of the pre-mission defined state. These maneuvers are executed by the on-board guidance and control systems. The navigation state estimates are also used to compute attitude maneuvers for the spacecraft so that scientific or navigation observations can be made.

Robotic Earth orbiting, planetary and lunar missions use ground-based navigation for providing the state estimates of the spacecraft. During the mission, the on-board systems provide the necessary attitude determination and control of the spacecraft for scientific and navigation **observations**, and for the orienting of the spacecraft so that ground-computed course correction

maneuvers can be executed. An on-board navigation Capability is provided for planetary and lunar landings. This system is initialized with ground-based state estimates at the start of the landing mission phase. Navigation measurement data is logged and used in combination with other ground and on-board sensor data for the accurate post-flight determination of the spacecraft landing state.

Manned missions use a ~~combination~~^{combination} of on-board and ground-based navigation systems. The on-board navigation ~~systems~~^{system} whose operation is controlled by the crew, contains the requisite navigation sensors and computing capability to successfully carry out the mission, independent of the ground, if **necessary**. During **nominal** mission operations, both ground and on-board navigation system capabilities are used. Depending on the mission phase and the availability and accuracy of sensor information, either the on-board or ground navigation solutions may be **prime** for maneuver targeting and guidance. The ground-based navigation system can provide periodic resetting of the on-board state estimates depending on mission phase. Post-flight, both on-board and ground navigation data **are** used for determining actual system accuracies and performance such that future mission capabilities **and** objectives can be expanded and successfully achieved.

Navigation systems for robotic and manned applications can and will differ in navigation techniques, accuracy and data latency **requirements**, system redundancy requirements, and in the location of the prime navigation system assets, ground or on board. These requirements also vary with mission phase: earth, **planetary** and **lunar** orbital coast, **trans-planetary** and **trans-lunar** coast, planetary and **lunar** operations and landing. In addition, the sensor configurations and the degree of on-board autonomy needed to achieve these requirements are different and also mission-phase dependent.

SECTION 3. NAVIGATION APPLICATIONS FOR ROBOTIC MISSIONS

Robotic spacecraft have performed a broad variety of functions during the past 25 years. Many spacecraft have been placed into orbit around the earth for a variety of commercial, military, and scientific purposes, including communication, navigation, **measurement** of the local space environment, and remote sensing of a broad **class** of man-made and natural objects throughout much of the electromagnetic **spectrum**. A number of robotic spacecraft have traveled throughout the solar system, collecting in-situ and remote scientific observations. In nearly all cases the ability to determine and control the flight path of the vehicle has been critical to mission success.

Robotic spacecraft have **travelled** in a broad variety of orbits, at distances from the earth's surface ranging from hundreds to billions of kilometers. Requirements on navigational accuracy have varied over a wide range, according to the general nature of each mission and the specific objectives to be accomplished. As a consequence, the navigational techniques employed have varied substantially also. Space limitations in this article do not permit a comprehensive coverage of all navigational techniques that have been used over the past 25 years for robotic spacecraft. Instead, the primary emphasis **will** be placed on a limited class of missions that have involved travel at great distances from the earth and, by their very nature, have pushed the development of many aspects of space navigation technology: the National Aeronautics and Space Administration's unmanned planetary missions launched from 1970 through 1994. Many earth-orbiting missions have been navigated using similar **techniques**, as will be pointed out.

3.1 History of NASA's Planetary Missions

To put the planetary missions of the past 25 years into context, it is worth reviewing first the history of **NASA's planetary missions** prior to 1970. During the 1960s the Ranger, Surveyor, and Lunar Orbiter series of missions were launched for the purposes of impacting the Moon, landing softly on the Moon, and photographing the Moon from orbit, respectively. These series of robotic missions were designed to acquire critical knowledge and experience that would be needed in the manned Apollo missions to follow. Beginning in 1959 several Pioneer missions were launched into heliocentric orbits to monitor the sun and measure properties of the interplanetary medium. In parallel with the unmanned lunar missions of the 1960s, the first unmanned planetary missions were launched: Mariner 2 to Venus in 1962, Mariner 4 to Mars in 1964, Mariner 5 to Venus in 1967, and Mariners 6 and 7 to Mars in 1969. Each of these early planetary missions involved a flyby of a planet, rather than an insertion into orbit or a landing, and had a single planetary destination.

With the start of the 1970s, the objectives in planetary missions became more complex. The Mariner 9 spacecraft, launched in 1971, was inserted into an elliptical orbit around Mars later that year [1]. In 1972 the first mission to the outer solar system, Pioneer 10, was launched; the spacecraft flew past Jupiter in 1973 [2]. The Pioneer 11 spacecraft, launched in 1973, flew past Jupiter in 1974 and Saturn in 1979, using the gravitational field of the former to allow passage by the latter [3]. These Pioneer spacecraft are still operating today and are traveling outward well beyond the orbit of Pluto in search of the heliopause where the magnetic influence of the solar system ends and the interstellar medium begins. Mariner 10, also launched in 1973, flew past Venus and used the Venusian gravity field to deflect the spacecraft's flight path inward toward Mercury [4]. The first flyby of Mercury was used to modify the spacecraft's orbital energy such that two more flybys of Mercury were possible.

Two Viking spacecraft, launched in 1975, were inserted into orbit around Mars and delivered descent vehicles to the Martian surface in 1976 [5]. In 1977 the two Voyager spacecraft were launched. Voyager 1 flew past Jupiter in 1979 and Saturn in 1980, Voyager 2 flew past Jupiter in 1979, Saturn in 1981, Uranus in 1986, and Neptune in 1989. Like Pioneers 10 and 11, Voyagers 1 and 2 are still functioning and are departing from the solar system, in search of the heliopause. In 1978, the Pioneer 12 and 13 spacecraft were launched toward Venus. Pioneer 12 carried four atmospheric entry probes, which entered various parts of the Venusian atmosphere [6]. Pioneer 13 was inserted into a 2.4-hour orbit around Venus, where it remained until entering the Venusian atmosphere in 1992 [7]. The ISEE-3 spacecraft was moved from its sun-earth libration point orbit in the early 1980s and sent past Comet Giacobini-Zinner, by means of a sequence of lunar gravity assist swingbys [8].

After an 11-year interval in which no U.S. planetary missions were launched, the Magellan and Galileo missions were launched in 1989. The Magellan spacecraft was inserted into an elliptical orbit around Venus in 1990, from which it mapped 99% of the Venusian surface with a synthetic aperture radar [9]. Late in the mission the orbit was reduced in size by using aerodynamic drag in the upper Venusian atmosphere, in order to more effectively carry out a gravity-field mapping experiment [10]. The mission was terminated in 1994 by allowing the orbit to decay into the atmosphere. In order to circumvent limitations in launch vehicle capabilities, the Galileo spacecraft was sent to Jupiter by means of one gravity assist flyby of Venus (in 1990) and two of earth (in 1990 and 1992) [11]. Two main-belt asteroids, 951-Gaspra and 243-Ida, were flown past in 1991 and 1993, respectively, on the way to Jupiter, which will be reached in 1995 [12]. The European Space Agency/NASA Ulysses spacecraft, launched in 1990, flew past Jupiter in 1992 and used Jupiter's gravity to place it in a high-inclination orbit about the sun, allowing observation of the sun's polar regions in 1994 and 1995 [13]. The Mars Observer spacecraft was launched in 1992. Communication with the spacecraft was lost in 1993, shortly before the planned insertion into orbit around Mars. The Clementine mission, a joint

venture between the Ballistic Missile Defense Organization and NASA, placed a spacecraft into a polar **orbit** around the moon for several months in 1994.

Although this section of the paper deals with the navigational techniques that have been used to fly NASA's **planetary** missions of the past 25 years, it should be noted that other nations have participated in the exploration of the **solar** system during this time and have used generally similar navigational techniques. A number of Soviet spacecraft have traveled to Venus and Mars. **The Soviet Union**, the **European Space Agency**, and Japan sent spacecraft to investigate Comet Halley in the mid- 1980s. The ESA spacecraft, **Giotto**, used a subsequent earth swingby to fly past Comet **Grigg-Skjellerup** in 1992. Japanese spacecraft have flown past or entered into orbit around the moon in recent years.

3.2 Navigational Objectives in Planetary Missions

All planetary missions involve an approach to at least one **celestial** body. That body may be simply flown past, or engines on board the vehicle may be fired to slow it down and place it into orbit around the body. In either case, measurements are acquired as the spacecraft approaches its *target*, and an orbit determination solution is obtained based on these data. This orbit determination process is repeated as additional measurements are acquired. Trajectory correction maneuvers are performed several times during the approach, if the predicted encounter conditions are not within some tolerance of the desired conditions. When the last allowable trajectory correction **maneuver has been** performed, typically several days before encounter, the delivery conditions are fixed and cannot be improved further. However, the collection of additional measurements and the generation of subsequent orbit determination solutions allows the trajectory to be predicted more accurately near encounter than it can be controlled. This allows the timing of spacecraft sequences and **the** pointing of instruments to be adjusted shortly before encounter to optimize the return of scientific data. Measurements that are collected around closest approach are received too late to either modify the encounter conditions or update instrument pointing, but are useful for deducing, after the fact, what the true encounter conditions were, **to** allow a best reconstructed orbit for scientific data correlation purposes.

Many planetary missions involve placing a spacecraft into orbit around some celestial body, rather than flying **by** (or impacting). In this scenario, the orbit of the spacecraft must be determined on a continuing basis, **to allow** both the correlation of scientific measurements with the locations at which they were recorded and the accurate pointing and sequencing of instruments in the future. In addition, some missions require that the orbit be controlled, so that the spacecraft flies over specific ground features, with specific lighting conditions, etc.

3.3 The Deep-Space Navigation System

The navigation system that has been used to perform **the** NASA robotic planetary missions described above includes the **Deep Space Network (DSN)**, elements of the spacecraft (principally for communication and imaging), ground-based computational facilities and software, and various support functions [14-16]. (See Fig. 3.) The various parts of the overall navigation system **will** be discussed in **the** subsections that follow.

3.3.1 Measurement Systems

The Deep Space Network consists of three complexes of large radio antennas, located at **Goldstone**, California; Canberra, Australia; and Madrid, Spain. **With** the complexes spread **between** the northern and southern hemispheres and relatively evenly spaced in longitude, any

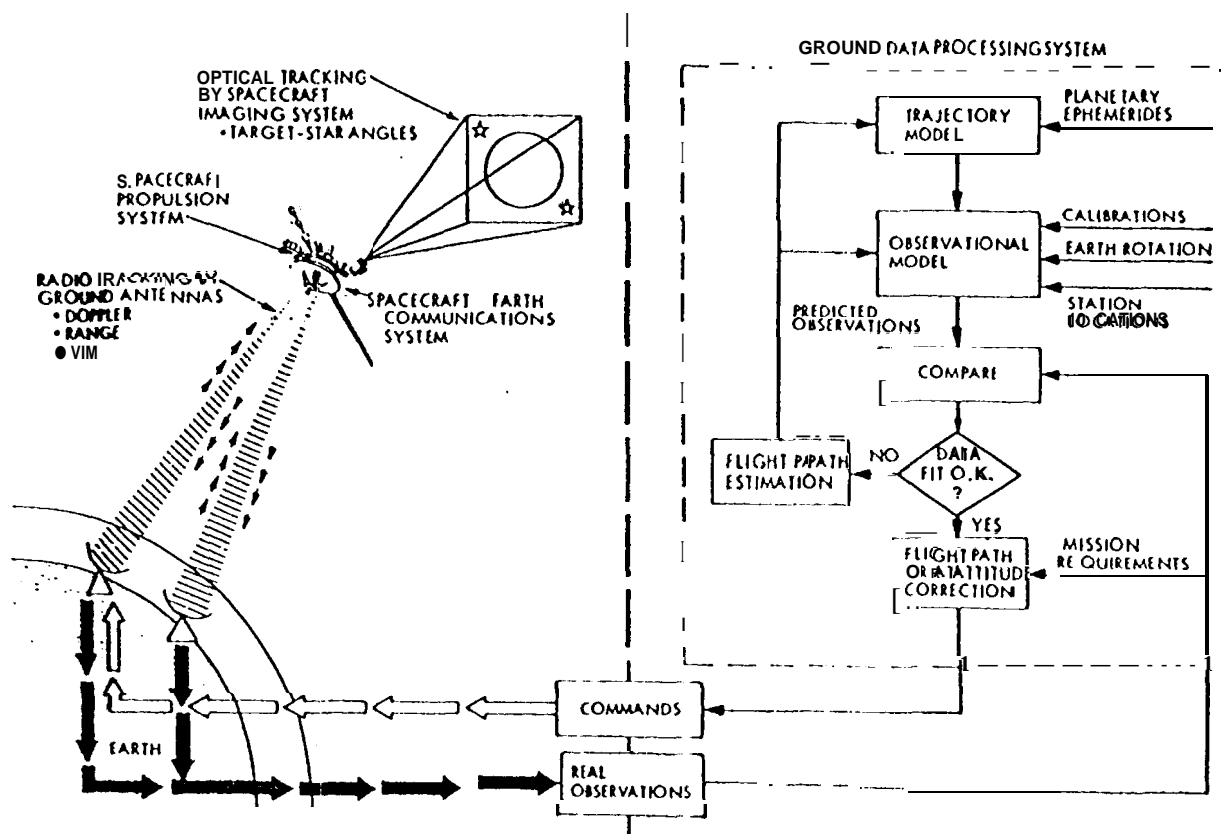


Figure 3. Deep Space Navigation System

planetary spacecraft can usually be seen from at least one tracking complex at any given time. (Planetary spacecraft usually lie reasonably close to the ecliptic plane, the plane of the earth's motion about the sun, and thus within about 30 degrees of the earth's equatorial plane.) Each complex currently includes one 70-m diameter antenna and several 34-m antennas that can be used for tracking planetary spacecraft. Several smaller antennas are also at each complex for tracking earth-orbiting spacecraft. Nearly all planetary spacecraft launched since 1970 have been able to communicate with the DSN at S-band (2.1 GHz uplink and 2.3 GHz downlink) frequencies. Most have also had an X-band (8.4 GHz) downlink capability. The most recent spacecraft have been able to receive X-band uplink frequencies (7.2 GHz).

The most fundamental radio navigation measurements in deep space missions are two-way Doppler and range, acquired at S- and X-band frequencies by the Deep Space Network. The Doppler shift is proportional to the spacecraft-station range rate and can be measured in 1-minute counts to an accuracy of about 2 mHz, which is equivalent to a range-rate precision of about 0.1 mm/s at X-band. (Random errors are expressed here and below in terms of their standard deviations.) Range, derived from the signal transit time, is measured to a few meters accuracy, assuming perfect knowledge of the velocity of the radio signal. (Two-way Doppler and range data are heavily relied upon in navigating many earth-orbiting missions, also.)

In recent years the technique of Very Long Baseline Interferometry (VLBI) has been developed for use as a navigation data source. VLBI measures the difference in signal reception

times at two widely separated ground stations to an accuracy of several nanoseconds. When compared with the signal reception time difference from a background **extragalactic** radio source (or quasar), **these** measurements allow the spacecraft direction to be determined to an accuracy of 30 nrad with **respect** to the direction to the background quasars.

Optical measurements can be obtained from the science imaging instruments on board planetary spacecraft. These optical instruments, designed to meet the stringent high-resolution and dynamic-range specifications required for scientific imaging of the planets and their natural satellites, have proved to be excellent for optical navigation. Images of the target planets and their satellites against star backgrounds yield valuable data for guidance during the approaches to these planets. Spacecraft angular position determination fixes to accuracies of 5 microrad or better are obtainable from these data.

3.3.2 Data-Processing Systems

Radio metric data (Doppler, range, and, when applicable, VLBI) are extracted from the incoming radio signals at the tracking stations. Optical data are digitally encoded on board the spacecraft and transmitted to earth using the same **downlink** signal from which radio navigation data are derived. All navigation data are then transmitted to a central facility at the Jet Propulsion Laboratory in Pasadena, California, and buffered in computer storage. A large software system is then used to compute the spacecraft orbit and, when appropriate, **trajectory-correction** maneuver parameters.

Newly acquired radio metric data are first **p**rocessed to form data blocks from different tracking stations, which are merged into a single, time-sequenced array. Data of poor quality are then removed, and the arrayed and edited data are made ready in computer storage for orbit-estimation processing.

Two major modules are used in the orbit-estimation process. The first is the **trajectory** module, which numerically integrates the trajectory (and state transition matrix partial derivatives) from assumed initial conditions, taking into account all known forces acting on the spacecraft that are large enough to be of consequence. The equations are developed in a Cartesian coordinate frame referenced to the earth's mean equator and equinox of 2000.0, and numerical integration is performed using a variable-order predictor-corrector method. A second large module computes simulated observable corresponding to each actual observation, based on the modeled trajectory, and computes the partial derivatives of the observable with respect to the initial conditions of the trajectory. It may also compute partial derivatives with respect to a multitude of additional trajectory and observational model parameters, such as those associated with a planet's gravity **field**, planetary position coordinates, spacecraft gas leak forces, and tracking-station locations [17, 18]. An array of observation residuals is formed, and an analysis is performed to produce a best estimate of corrections to the initial state and other parameters. (Similar software, with some differences in modeling complexity, is used to determine orbits for many earth-orbiting missions.) The estimation algorithm used may be straightforward least-squares or sequential in nature, with stochastic accelerations of the spacecraft modeled if desired. The estimation process can be repeated iteratively until convergence is obtained, and the final product of the estimation process is a numerically integrated trajectory that best fits the observations. During the 1970s and early 1980s, these computations were carried out in a large mainframe computer. During the 1980s the orbit determination software, which contains more than a million lines of code, was transported to minicomputers, with the software maintained in both operating environments to fulfill the desires of various **flight** projects. During the 1990s a further migration has taken place to high-performance work stations.

Optical data are first processed in a man-machine interactive system, where full-frame images from the spacecraft are displayed on a **videographics** screen. There, an analyst can identify **the** target body and **the** background stars in the image. **Limb-fitting** algorithms are employed to locate the geometric center of the target body. The optical observable are then formed as the distances on the image plane between the target center and the identified stars. Dividing these distances by the camera focal length produces a measure of the angles between the target and the stars. Simulated observable and partial derivatives of the optical observations with respect to the spacecraft state and other parameters such as the target location and camera biases are then computed. An optical data file of the observable residuals and partial derivatives is produced, which is merged with the radio data files. Joint orbit estimates based on both radio and optical data can then be computed.

The best estimate of the spacecraft trajectory, derived from radio metric data throughout a mission and radio metric plus optical data near an encounter, serves as the basis for computation of the velocity **-correction** parameters. Computation of these parameters is performed in another software module, often taking into account an evolving redesign of the remainder of the mission. The effects of all maneuvers on the future flight path, the science viewing geometries it produces, and the resulting predicted propellant expenditure are usually verified by simulation studies before a maneuver is executed.

The high accuracy required for deep-space navigation is achieved with precise observational measurements and precise knowledge of the timing of these measurements, numerically accurate computational algorithms, and a precise modeling of **all** physical phenomena that affect the values of the observational measurements. These phenomena include those that affect the measurements directly and those that affect the measurements through their influence on the motion of the spacecraft. Examples of phenomena that require highly accurate knowledge include the locations of the tracking stations on the earth, the earth's rotational motion, the motions of the earth, moon, planets, and their natural satellites through the solar system, the gravity-field **structures** of the earth and other massive bodies, and the effects of the transmission media on the radio signal. All of these phenomena are modeled in the **orbit-determination** software. Many require separate, off-line support activities to provide parameter values of the needed accuracy. Brief descriptions of these support functions are provided in the following subsection.

3.3.3 *Navigation Support Functions*

Position coordinates of the Deep Space Network tracking stations in California, Spain, and Australia have historically been computed in the orbit-determination software from Doppler data taken during the planetary encounters of the past 30 years. The locations of the stations are therefore **computationally** tied to the planets, which is logical since the purpose of locating them precisely is to navigate spacecraft to the planets. A large and expanding data base of **planetary-encounter** Doppler data is maintained. As a new planetary ephemeris is generated, or as new encounter data become available, the locations of the earth tracking stations are recomputed. In recent years **VLBI** measurements have enabled a considerable improvement in station location accuracies. Stations are presently located relative to the earth's crust to within an uncertainty of **10** cm, more than an order of magnitude improvement since the 1970s.

The earth's precessional and notational motions can be computed by mathematical series expansions, the parameters of which have been determined from centuries of astrometric observations. Universal time and polar motion data have been obtained from the Bureau **Internationale de l'Heure** based on its reduction of meridian circle data over much of the past 25 years. These earth rotational variations are stored in computer files in polynomial form and are applied as calibrations to the computed radio observables. In recent years **VLBI** observations

have enabled the earth's poles to be located to a 10-cm accuracy and the earth's rotation **angle** about its polar axis to be determined to **0.5** ms, as measured by universal time.

Tropospheric effects on Doppler and range data are modeled by equations that include variations in signal elevation angle, local humidity, and temperature. Charged-particle effects from the earth's ionosphere are modeled as elevation-dependent daily varying calibrations, the values of which can be computed using Faraday rotation data from satellites in **geostationary** orbit. The effects of charged particles along a signal path can also be calibrated directly by analyzing the difference in their effects on the **downlink** Doppler data at two frequencies received from the spacecraft of interest, assuming that both S- and X-band **downlinks** are available. X-band radio metric data are much less affected by plasma interactions than S-band data because of the inverse-square frequency dependence of these interactions. Thus, the movement toward higher telecommunication frequencies over the past 25 years has reduced ionospheric- and space plasma-induced errors substantially.

Over the past 25 years **planetary** ephemerides have been derived primarily from optical transit and other **astrometric** data acquired using earth-based telescopes over the past century, radar ranging of several planets and planetary satellites using the Goldstone Solar System Radar over the past several decades, lunar laser ranging, and spacecraft radio metric and optical data acquired during planetary missions. A data-reduction software system is maintained to process these observations and produce highly accurate ephemerides. Planetary ephemerides have improved significantly over the past 25 years, as new measurement techniques and more data have become available. Current earth-relative ephemeris accuracies vary from about 100 to 500 **nrad**, with inner planets having much smaller ephemeris uncertainties than outer planets, asteroids, and comets. Ephemerides for the planets' natural satellites are generated in separate software systems and were initially developed **almost** exclusively from astrometric plate measurements. Television images of the satellites of Jupiter, Saturn, Uranus, and Neptune acquired by **the** Voyager cameras now contribute to the data base. The motions of **natural** satellites in complex, multi-body gravitational systems can be predicted analytically or by numerical integration.

The gravity-field structure of planets and their satellites is modeled by a potential function expressed as a spherical harmonic expansion. The expansion coefficients are determined most accurately from the Doppler tracking of spacecraft that have orbited or flown past these bodies.

3.4 Navigational Accuracy

Navigational accuracy for interplanetary flight can be characterized by the uncertainty with which a spacecraft is delivered to its target. The delivery error to a planet or distant satellite is usually comprised almost totally of the target-relative orbit determination error. Generally, maneuvers are performed shortly before target encounters, and position errors due to both maneuver magnitude and direction errors normally do not have time to increase appreciably before the encounter is achieved. In the following subsections, the orbit determination accuracies that are achieved using Doppler and ranging radio observations, VLBI observations, and on-board optical observations are examined.

3.4.1 *Doppler and Ranging Observations*

Doppler measurements constituted the first observable employed for the determination of spacecraft orbits in deep-space missions. The Deep Space Network generates two-way Doppler measurements of **extremely** high precision and stability. The measurements are

provided in the form of a nondestructive count (in cycles) of the integrated frequency difference between a Doppler reference frequency transmitted to the spacecraft and the frequency that is returned from the spacecraft (with an adjustment made for the frequency multiplication that takes place in the spacecraft transponder). The Doppler measurements are therefore proportional to the spacecraft-station velocity resolved along the line of sight.

The network also uses a binary-coded, sequential-acquisition ranging technique to provide a measurement of the round-trip light travel time between the station and the spacecraft. This measurement is proportional to the **line-of-sight** range.

For a distant spacecraft, the station-relative range rate is approximately **equal** to the geocentric range rate plus a **sinusoidally** varying term associated with the earth's rotation. (See Fig. 4.) The phase of the sinusoidal signal is linearly related to the right ascension of the spacecraft (the angle from the **vernal** equinox direction to the projection of the spacecraft's position vector onto the earth's equatorial plane), and the amplitude is proportional to the cosine of **the** spacecraft's geocentric declination (the angle between the spacecraft's position vector and the equatorial plane) [19]. Thus, a time series of Doppler data can be used to infer the direction to the spacecraft, in terms of **its** right ascension and the cosine of its declination. The sensitivity of the Doppler data to the declination is proportional to the sine of the declination, which causes a degradation in orbit determination accuracy at low declinations. The accuracy of the determination of right ascension is not particularly sensitive to variations in geometry.

An obvious concern therefore develops if a target planet is near zero declination when **encountered** by a spacecraft. In the **context** of the simple model described above, a singularity occurs, and the Doppler-based orbit **determination** uncertainties in declination increase sharply. However, if two stations with a long north-south baseline measure the range, errors in the measured range difference are proportional to the reciprocal of the cosine of the declination, not the reciprocal of the sine; and no singularity occurs at zero declination. The planetary ranging system produces deep-space range measurements accurate to a few meters, so that a two-station range difference involving stations in California and Australia, with a north-south baseline of 5000 km, can provide a direct measurement of spacecraft declination to about 500 **nrad**. At moderate and high declinations, Doppler data can do as **well** as 100-200 nrad, but the difference range measurement provides a 500-nrad error bound at low declinations. Right ascension is usually determined to within 100-200 nrad for all geometries. At the distance of Jupiter this angular uncertainty translates to a position uncertainty of 75-150 km. The position uncertainty lies predominantly in a **plane perpendicular** to the earth-spacecraft **line**, since range measurements directly **determine** the **line-of-sight** component of position much more accurately. The errors stated above are for the **early** 1990s. During the 1970s and early 1980s position determination errors of 250 nrad at high declinations were typical using Doppler data.

Achieving these accuracies requires precise modeling and computation in the navigation data-processing **system**. Submeter observable modeling is employed throughout the navigation processing system, which demands in turn the use of several model support systems described above, which furnish data and constants necessary for accurate computation. Submeter modeling has been achieved by the use of double precision (at least 16 significant figures) in all trajectory and observable computations, and **the** use of a relativistic light-time solution algorithm in the Doppler and range observable computations. This algorithm takes into account the retardation in the velocity of **light** by gravity and the transformation from solar-system **barycentric** coordinate time to earth-station proper time [17].

Realized navigation accuracy is, of course, different from mission to mission, depending , on the particular mission geometry and **often** on the number and severity of unusual occurrences **during** the flight. Factors that influence a realized navigation error include disturbances in

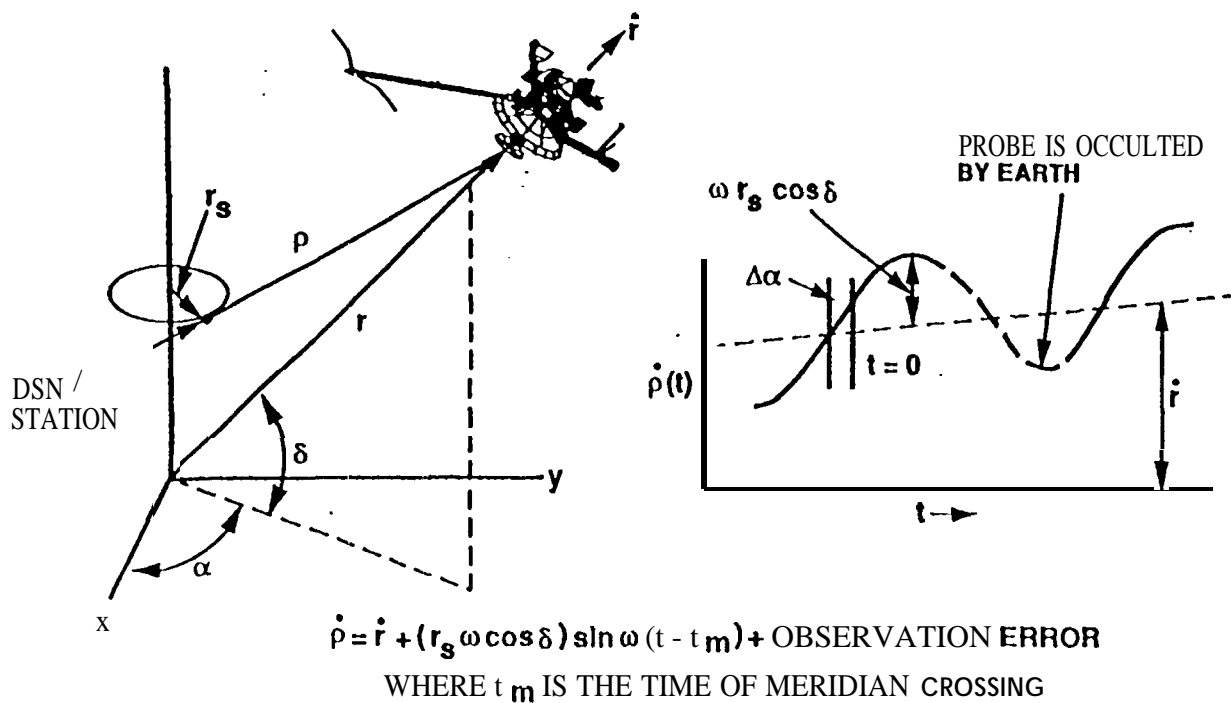


Figure 4. Characteristics of Doppler as a Deep Space Navigation Measurement.

transmission media that affect radio metric data, unanticipated forces that unexpectedly accelerate the spacecraft, and errors in target location, to name a few.

This discussion applies to cruise and distant approach phases of planetary missions. Once a spacecraft is well within the gravitational field of a distant body, whether flying by or as a captured satellite, its orbit can be computed more accurately from Doppler data than it can be computed during the cruise. The strong gravitational attraction of the body allows this. Orbits are determined, for instance, to within a few kilometers for artificial satellites of Mars and Venus.

Although Doppler and ranging data are used to determine orbits of earth-orbiting, as well as planetary, spacecraft, the information content of the data is quite different in the two cases. Earth-orbiting spacecraft change rapidly in angular position relative to the earth, whereas planetary spacecraft move very slowly. This difference makes the signature of the earth's rotational motion very important when tracking planetary spacecraft and much less so for earth-orbiting spacecraft.

3.4.2 VLBI Observations

The generation of Doppler and range measurements requires only a single tracking station and a closed signal loop from the station to the spacecraft and back to the station. Very long baseline interferometry observations, however, require the radio signal produced by the spacecraft to be received and recorded simultaneously at two radio antennas. Because of a difference in ray paths, the signal arrives at one antenna some time after it reaches the other. By

cross-correlating the two recorded signals, this time delay and/or its time derivative may be determined with great precision. Very long baseline **interferometry** measurements can also be generated from the radio signals from background natural **extragalactic** radio sources, which may be regarded as fixed objects because of their great distances,

The differential VLB1 observable thus involves the simultaneous tracking of first a spacecraft and then a nearby **extragalactic** radio source from two widely separated ground stations [20]. Through the correlation processing of the spacecraft data, the difference between the times the two stations receive the same signal can be computed to a few ns. The same correlation process is applied to quasar data, and a similar time delay is obtained. Both computed time delays **are** sensitive in **almost** the same way to station location, transmission media, timekeeping, **and** instrumentation errors. If the respective time delays are difference, the resulting doubly difference delay, referred to as Delta-Differential One-Way Ranging (**Delta-DOR**), is relatively insensitive to these major error sources. The **double-differencing** technique provides a spacecraft direction-angle fix that is accurate to 30 nrad relative to the observed quasar.

NASA's Galileo mission spacecraft transponder was designed to generate modulated side bands at S- and X-band. **The** most widely separated side tone is at 19 MHz for X-band and approximately 4 MHz for S-band. The process of determining the time delay from these signals with Delta-DOR is achieved by using multiple narrow-band channels. The phases of the **radio-frequency** side tones at the lower and upper 19-MHz signal frequencies are measured, and when this information is divided by the wide bandwidth separation of these tones (38 MHz), then the group delay or time delay of the transmitted signal is determined. The intermediate side tones between the extreme 19-MHz side tones serve to resolve the phase ambiguity in the measurement of the widely separated side tones. (The 38-MHz bandwidth is not currently available in the Galileo mission because the high-gain, X-band antenna has not deployed properly.)

Delta-DOR is thus a **downlink-only**, doubly difference range system that requires short, 10-rein passes of data during station view-period overlaps and is accurate to about 30 nrad. A total navigation **accuracy consistent** with the 30-nrad Delta-DOR measurement accuracy is achievable only **if** the **positions** of the target planets and satellites are known to that same accuracy with respect to the quasar locations. Today the planet-to-radio-source coordinate frame tie is accurate to 50-200 nrad, with the frame tie better for inner than for outer planets.

3.4.3 *Optical Observations*

In the last few months before its encounter with a distant planet, a spacecraft's orbit accuracy can be **improved** with optical data. The navigational accuracies achievable with optical data must be characterized differently than those associated with radio metric data. The optical observation is target-relative rather than earth-based, a considerable advantage since the effects of the target-relative **ephemeris errors** are minimized, and the spacecraft is much closer to the target than to the earth when the **final** flight-path delivery maneuvers are performed. Since the optical observable measures angles directly, the strength of the observable is relatively insensitive to changes in trajectory-target geometry, unlike Doppler data. A limiting error is the resolution of the camera. Line and pixel (picture element) spacings in the Voyager vidicon and Galileo charge-coupled **device** imaging systems are about 0.015 mm, and the optical focal lengths are 1.5 m. Therefore, half-pixel resolution produces an angular resolution of 5 **microradian**. The ultimate positional accuracy obtainable with optical data is limited by the **ability to determine the gravitational center of the target body from the limb and terminator measurements in the optical images**. The centerfinding capability has been found to be better than 1 percent of target-body radius for regularly shaped objects.

μ (mm)
The **5-microradian** accurate angle data provide orbits good to about 1 km for every 200,000 km distance from the target body. Since approach speeds are typically around 10 km/s, optical data are useful for improving radio-determined orbits over the final month or so before a planetary encounter. In the final week before an encounter, the flight path can often be predicted to the point of closest planetary approach with an accuracy close to 10 km.

The accuracy of radio navigation is characterized by the uncertainty in the direction to the spacecraft as viewed from the earth, using Doppler, range, and perhaps Delta-DOR measurements. Earth-based radio navigation and its less accurate but target-relative counterpart, optical navigation, form complementary measurement sources, which provide a powerful sensory system to determine accurately the orbits of planetary spacecraft.

3.5 Planetary Mission Applications

The following subsections will describe how the deep-space navigation techniques described above have been used in several very demanding planetary encounters - the Voyager encounters with Jupiter, Saturn, Uranus, and Neptune, and their systems of natural satellites and rings.

3.5.1 Voyager Navigation at Jupiter and Saturn

The two Voyager spacecraft were launched in the summer of 1977. Voyager 1 arrived at Jupiter in March of 1979 and passed within 350,000 km of the planet, while being targeted to a close (20,000-km) flyby of the satellite Io. Voyager 2 encountered Jupiter in July of 1979, passing within 730,000 km of the planet and encountering the satellite Ganymede at a distance of 62,000 km. (All distances are measured from the centers of the various bodies.) Voyager navigation at Jupiter is discussed in [21].

Voyager 1 flew by Saturn on November 12, 1980. The flight path was targeted such that the spacecraft flew within 7000 km of Titan, 18 hours before closest approach to Saturn. After the close encounter with Titan, the flight path passed directly behind the satellite, as viewed from the earth, which allowed the atmosphere of Titan to affect the radio signal, and thus provide data for atmospheric studies. The spacecraft then passed close by (185,000 km), and then behind, Saturn and its rings, so that similar effects on the radio signal due to the planetary atmosphere and ring system could result. The spacecraft then continued on out of the Saturnian system, passing through the E-ring and making imaging passes by several Saturnian satellites, the closest approach being relative to Rhea (73,000 km).

Voyager 1 was required to perform a diametric earth occultation with Titan to within a tolerance of 265 km and then, after closest approach to Saturn, to pass through a 5000-km wide corridor in the E-ring, where it was believed that particles have been swept away by the satellite Dione, and the chances of a disastrous impact consequently minimized. The close encounter with Titan created a difficult navigational challenge for controlling the instrument pointing for observations of the Saturnian satellites on the outbound leg of the Saturnian system encounter. Uncertainties in the dispersed flight path after the Titan and Saturn flybys made it mandatory to quickly and accurately redetermine the trajectory after the Titan closest approach.

Optical navigation was required for the first time in the Voyager mission to meet a deep space mission's objectives. (It had been demonstrated previously in several Mariner missions and the Viking mission and had improved the orbit determination accuracy, but it had not been essential to mission success - radio metric orbit determination accuracy had been entirely adequate.) The radio Doppler system was used as the baseline cruise system, but optical measurements were employed over the final few months before each encounter and served as the

most accurate navigation measurements for the planetary encounters. The Doppler system served as an initialization and backup to optical navigation during the Jupiter approaches. The Doppler system, augmented with the two-station range measurement system, was adopted as a backup at Saturn [22]. (The Voyager 1 encounter with Saturn occurred near zero **declination**, motivating the development of the two-station ranging technique.) Optical navigation was performed in the Voyager mission using images of the satellites of Jupiter and Saturn, not the planets themselves. The smaller sizes of the satellites and their clearly defined surfaces made them more attractive as optical navigation targets than the central planets. In addition, many of the encounter target conditions were relative to the satellites themselves, so that knowledge of the flight path of the target satellite was required to the same accuracy as the spacecraft flight path.

Special-purpose satellite ephemeris propagation software for the **Galilean** and **Saturnian** satellite systems was developed, and an extensive **pre-encounter** ephemeris generation activity, including the acquisition of many new **astrometric** plate observations, was undertaken. The ephemeris-propagation software was also used in the flight navigation system, and the satellite ephemerides were corrected as the spacecraft orbit was determined from the optical navigation measurements,

The Voyager 1 encounter with Saturn was, from the standpoint of navigation, the most complex planetary encounter experienced up to that time. The analytical theory-based Saturn satellite ephemeris propagator, used for the preflight ephemeris generation, was not accurate enough for the reduction of optical measurements of Titan. Therefore, the preflight Titan **ephemeris** theory parameters had to be transformed to a **Cartesian** state vector, and the subsequent path of Titan numerically integrated [23]. Many spacecraft orbit solutions were processed and reviewed during the approach to Titan before a final, successful one was chosen. Voyager achieved its flyby of Titan by means of two trajectory correction maneuvers, performed 33 days and 5 days before encounter. The flight path was accurate to 330 km, with the error only 37 **km** in the most important direction, allowing a nearly perfect **diametrical** occultation by Titan to be achieved.

During the Titan encounter, Doppler data, which were then greatly influenced by Titan and hence very sensitive to the flyby distance and Titan's mass, were processed to quickly determine the flyby trajectory to high precision. This action led to accurate instrument-pointing adjustments for the outbound imaging of the satellites **Mimas**, **Enceladus**, **Dione**, and **Rhea**. The delivery to **Titan** was also sufficiently accurate that the spacecraft passed safely through the presumed gap in the E-ring created by **Dione** on its escape from the Saturnian system.

The primary concern in the navigation of Voyager 2 to Jupiter and Saturn was the retention of adequate propellant to reach Uranus. During a planetary swingby, an error in either the approach trajectory or the mass of the planet leads to an error in the outbound direction of travel, which must be corrected with a propulsive maneuver. This maneuver reduces the remaining propellant available for both attitude control and subsequent flight path corrections.

Voyager 2 encountered the Saturnian system on August 25, 1981. The spacecraft passed by Saturn at a distance of 161,000 km and then passed within 100,000 km of the Saturnian satellites **Enceladus** and **Tethys**. The Voyager 2 navigation requirements at Saturn were neither as stringent nor as complex as those of Voyager 1. The incoming trajectory was controlled quite accurately, resulting in small corrective maneuvers after the encounter and leaving ample propellant for future use.

The Voyager navigation experience at Saturn brought to reliable maturity the optical navigation process. The two-station range backup system, although a wise investment in overall mission reliability, did not make a critical contribution to orbit determination accuracy, because

of the outstanding **performance** of the optical navigation process. Further information about the navigation of the Voyager encounters with Saturn may be found in [24].

3.5.2 Voyager-2 Navigation at Uranus and Neptune

The navigational challenges in the Uranus and Neptune encounters were similar in some respects to those in the Jupiter and Saturn **encounters**, but certain **new** problems arose in addition. Due to the greater geocentric distances of Uranus and Neptune, ephemeris uncertainties for these bodies and their natural satellites, based on telescopic observations from earth, were significantly larger than for Jupiter and Saturn. **Pre-encounter** ephemeris errors for Uranus, Neptune, and **Triton** (relative to Neptune) were about 5000, 10,000, and 6700 km, respectively. Corresponding a priori ephemeris errors for Jupiter and Saturn had been only 400 and 800 km. An effort was undertaken for several years to improve the ephemerides of Uranus, Neptune, and their satellites by expanding the observational data base and using suitable dynamical modeling techniques [25,26]. Even with some improvement in these earth-based ephemerides, however, on-board optical data were extremely important for accurate prediction and control of the spacecraft's trajectory relative to these far outer planets and their satellites.

On-board optical data are quite effective in determining the position components of a spacecraft that are perpendicular to its nominal flight path in a target-body centered reference frame, but they yield relatively little information about the position along the flight path until quite close to encounter. Radio metric data can be helpful in estimating these time-of-flight errors by sensing the gravitational field of the target planet. Time-of-flight errors tended to remain quite large in the approaches to Uranus and Neptune, however, for several reasons: 1) the masses of Uranus and Neptune are smaller than **those** of Jupiter and Saturn, and the approach speeds were higher in the encounters with the former, so that the gravitational fields of Uranus and Neptune did not exert a significant influence on the trajectory until relatively close to **encounter**; 2) the encounters occurred at large negative geocentric declinations, so that relatively little tracking data could be gathered at the two Deep Space Network tracking complexes that **are** located in the northern hemisphere; and 3) the very long round-trip light times of 5.5 **hr** at Uranus and 8.3 **hr** at Neptune **substantially reduced the amount of two-way, coherent tracking data that could be collected.**

The use of **Delta-DOR** data offered a means of reducing the impacts of these adverse factors. Only short periods of overlapping station **coverage** were needed for accurate geocentric angle determination using **Delta-DOR** techniques. Thus, limited tracking coverage at the northern hemispheric stations was not a serious problem. Moreover, Delta-DOR is a one-way data type, so that the round-trip light time is not particularly important.

Utilization of the full potential of Delta-DOR data for orbit determination requires a wide-band transponder on board the spacecraft. The Voyager spacecraft transponder was not designed to have a wide bandwidth. However, the 360-kHz square-wave telemetry subcarrier used to modulate the S- and X-band downlink carriers could be used to generate a signal of adequate bandwidth. Observation of the **fifth** harmonics of the telemetry subcarrier, centered about the **downlink** carrier frequency, produced a spanned bandwidth of 3.6 MHz, for example. Due to bandwidth limitations, the **Delta-DOR** data that could be obtained in this manner were not accurate to the 30-nrad performance level mentioned earlier. However, the data were still quite useful in both encounter and cruise phases.

The nominal encounter geometry was such that both geocentric and heliocentric occultations of the spacecraft by Uranus were virtually guaranteed. The closest satellite **encounter** was with Miranda, at a distance of less than 30,000 km. Since the uncertainty in time of flight did not diminish appreciably until relatively close to **encounter**, errors in arrival time would have been **relatively** expensive to correct, in terms of propellant consumption, once they

were finally known. As a consequence, the final trajectory correction maneuver was used to control the position perpendicular to the direction of relative motion, but not time of flight. The controlling of two, rather than **three**, encounter parameters resulted **in** a considerable propellant savings but necessitated a late adjustment in the timing of data-collection sequences. Extremely accurate approach navigation allowed a mosaic of high-resolution images of Miranda to be obtained. Further information about the navigation of the Voyager encounter with Uranus may **be** found in [27-29].

The nominal flyby geometry at Neptune was subject to fewer constraints than at Uranus, there **being** no subsequent planet to encounter, **leavi** ng more options available for encounter geometry. Geocentric and heliocentric occultations of the spacecraft by Neptune could be easily achieved. Similar occultations by Neptune's satellite **Triton were** also strongly desired, but presented a much greater navigational challenge due to the much smaller size of **Triton**.

Concerns for spacecraft safety led to requirements that the vehicle pass no closer than 28,680 km from the center of Neptune at the time of closest approach (to avoid the outermost portions of Neptune's atmosphere) and no closer than 73,500 km from the center when crossing Neptune's equatorial plane (to avoid collisions with particles in Neptune's rings). In order to fly past **Triton** at the desired closest-approach distance of 40,000 km, it was first thought necessary that these Neptune-relative distances be 29,180 km and 78,400 km, respectively. The safety margin of 500 km in closest-approach distance to Neptune was judged acceptable, because it was felt that this quantity could be controlled to an error standard deviation of 150 km. Refinement of the estimates of the mass of Neptune, the orientation of its spin axis, and the ephemeris of **Triton** as the encounter became closer caused the nominal distances at Neptune's ring plane crossing and closest approach to shift somewhat, in order to hold the closest approach distance to **Triton** constant at 40,000 km, but did not erode the safety margins significantly.

The achievement of occultations of both the sun and the earth by **Triton** was more difficult than achieving either occultation alone. In addition, estimates of the radius of **Triton** were revised downward from well over 2000 km to less than 1600 km and ultimately to 1360 km, as the encounter became closer, increasing the flight path accuracy required to achieve the dual occultation. Accurate prediction of the flight path was also required during the passage through **the Neptunian** system in order to point the cameras accurately at **Triton** and other natural satellites (some of which were discovered as the encounter unfolded) and in order to point the spacecraft antenna properly during the occultation of the earth by Neptune. The radio science limb tracking experiment required shifting the direction in which the high-gain antenna was pointing as the radio signal penetrated deeper in the **Neptunian** atmosphere and was refracted through a greater angle, in order for the signal to be headed toward the earth upon exiting the atmosphere.

All of these requirements on navigational accuracy were met, resulting in a remarkable return of scientific data from this first-ever encounter with Neptune. The safety requirements were met by delivering the spacecraft to a Neptune closest approach radius of 29,240 km, just 90 km outside the revised nominal distance and 560 km outside the minimum safe distance. The distance at the time of ring-plane crossing was 85,300 km, easing any concern about ring particle impacts, and in accordance with an outward shift in the nominal distance due to a revised estimate of Neptune's pole orientation (and correspondingly, the location of the ring plane). The desired **aimpoint** in the **Triton** dual occultation zone was achieved to within 220 km, a small error given that the **Triton** encounter occurred about 5 **h** after the close passage over Neptune's polar regions, with errors on approach to Neptune **tending** to be substantially magnified by the gravitational bending of the flight path. The time of arrival at Neptune was controlled well enough (260 s) by the first of three **planned approach** trajectory-correction maneuvers that the second **scheduled** maneuver could be omitted, **eliminating** a subsequent two-day outage of two-way Doppler data, due to extreme temperature **sensitivity** on the part of the partially failed

spacecraft receiver. The third scheduled trajectory correction maneuver was made with attitude control thrusters, which avoided the heating problem and provided the final correction needed to achieve the dual occultations by Triton.

Around the time of closest approach to Neptune, the spacecraft position was predicted to an accuracy of 40 km and the time of arrival to 0.6 s. Late updates to instrument and antenna pointing sequences were made based on the most current orbit determination solutions. As a consequence, in the radio science limb tracking experiment, coherent Doppler data were collected down to below the 3-bar level in Neptune's atmosphere. Further information about the navigation of the Voyager encounter with Neptune may be found in [30-33].

SECTION 4. NAVIGATION APPLICATIONS FOR MANNED MISSIONS

Navigation for manned missions is provided by ground-based systems and by systems on board the vehicle. Both systems determine the vehicle position and velocity throughout the course of the mission. The primacy of either the ground or on-board navigation solutions is determined by the availability of navigation sensor data and the relative accuracy of the ground and on-board solutions computed using these navigation sensors. The navigation methods employed by the ground are essentially independent of mission phase, consisting of the processing of radiometric range, Doppler, and, if available, angle measurements from the ground antennas to the spacecraft. On-board navigation techniques, however, are dependent on mission phase. Before examining ground and on-board systems and their applications to manned programs of the last twenty-five years, it is instructive to review the key technology developments that enabled the development of an on-board Self-contained navigation capability.

4.1 Key Technology Developments That Made On-Board Space Navigation Possible

4.1.1 *Digital Computers and Miniaturization of Electronic Systems Components*

One of the most important technology developments that made on-board navigation possible was the development and extensive application of the all-electronic digital computer. Digital computers were initially used in military systems where the overriding factor in system requirements was the accuracy and speed of computation. Military weapons systems associated with weapons fire control, with aircraft and strategic missile inertial navigation and guidance, and with strategic missiles weapons delivery, used digital system mechanizations for performing the necessary navigation, guidance and control functions.

During the late 1950's and early 1960's, rapid developments in digital computer technology occurred. Micro-electronic integrated circuits and micro-miniature magnetic core memories for digital computers were introduced. This new technology resulted in digital computers with smaller volume, lower power requirements and higher speed. The application of the digital computer went beyond that of providing improved system accuracy. Complex mission functions such as failure detection and warning, status indications and backup mechanization and switching, became simple and inexpensive to implement. Between 1960 and 1970 alone, the equivalent cost of computers was reduced by a factor of eight. In addition, reliability was improved by a factor of twelve, power requirements were reduced by a factor of four, weight was reduced by a factor of ten and volume was reduced by a factor of 100. This improvement in digital computer capabilities enabled the use of the computer for additional aerospace navigation functions; inertial navigation aided with external observations; optimal

filtering, display interfaces, system status and reconfiguration; and enhanced spacecraft navigation applications [33, 34].

4.1.2 Inertial Measurement Unit (IMU)

The development of and improvement in the accuracy and reliability of inertial navigation systems also played a key part in enabling the development of space-based navigation systems for manned mission applications. A gimballed inertial measurement unit (IMU), such as the one used in the Apollo program, is shown in Figure 5. It has three gyroscopes and three accelerometers on an inner, or stable, platform which is isolated from vehicle motion by a set of gimbals as shown. The inner platform is kept stabilized in an inertial or fixed orientation relative to an inertial reference frame fixed to the celestial sphere (not moving with respect to the stars) using information from the gyroscopes. Spacecraft attitude relative to the inertial frame can be calculated using gimbal angle readouts of the body attitude relative to the inertial unit. The vehicle position in the inertial frame is determined using accelerometer measurements of the non-gravitational specific force arising from propulsion system maneuvers or aerodynamic forces, in integrating the equations of motion [35].

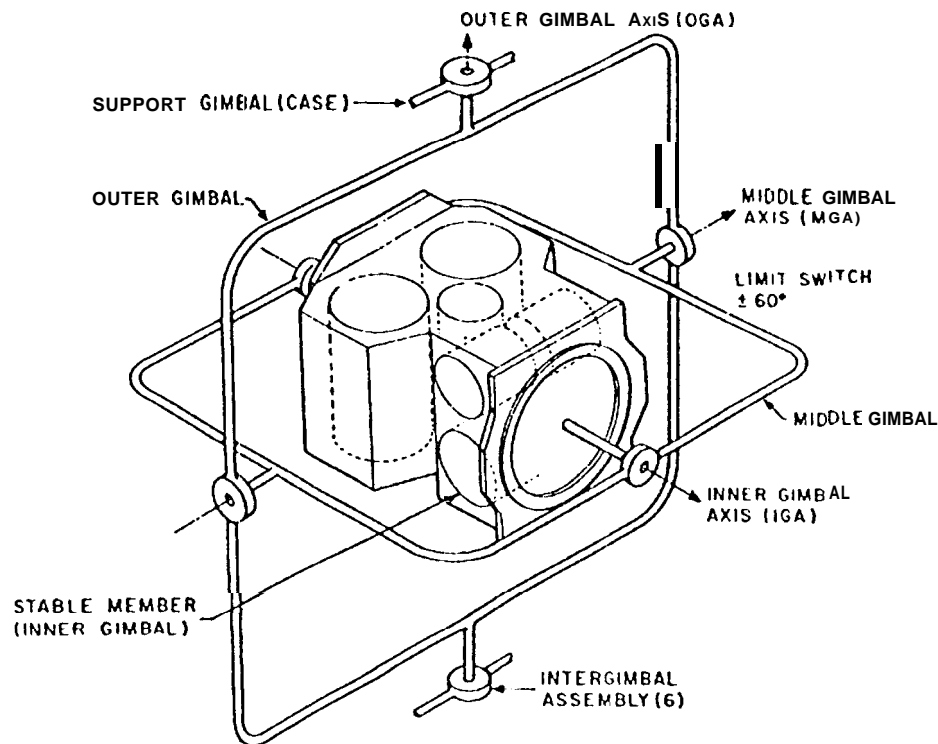


Figure 5. Inertial Measurement Unit

Precision attitude measurement systems using the properties of gyroscopes were initially used in military fire control systems. With the addition of gimbals for vehicle motion isolation and accelerometers mounted on the stable platform, inertial measurement units for determining accurate vehicle attitude, position and velocity were developed for aircraft navigation and for

enhancing military weapon delivery systems. With further improvements in accuracy and reliability, inertial measurement units **became** the key navigation instrument for missile systems. It was the development of these inertial measurement systems for missile applications that enabled the use of this key technology in manned space system applications.

4.1.3 Development of *Kalman Filter Theory and Recursive Navigation*

The development of the **Kalman** filter recursive navigation capability provided a method for improving the estimate of the spacecraft position and velocity by processing navigation measurement data from independent sources in a sequential or recursive manner. This sequential measurement processing capability avoided the numerical difficulties associated with **the least-squares** method of obtaining a navigation fix, which **was** used to provide navigation estimates at that time. The least-squares method required a matrix inversion after a sufficient number of measurements were made to obtain the six elements of **the** spacecraft state. These measurements were processed simultaneously, providing the best **fit** to all the data. For some applications, manual examination of the data was used to delete measurements from the solution, in an attempt to improve the state estimates.

The **Kalman** filter recursive navigation **capability** however, enables the use of sensor measurement data, one-by one, as it becomes available. Optimum measurement scheduling and selection of the measurement types to provide the best reduction in state estimation error could be determined from **pre-mission** analysis. Since one of the steps in the measurement data processing involves comparing the actual measurement with its estimated value determined from the current vehicle state, a reasonableness check on the quality of the measurement data is also easily made using this technique, thus providing an automatic capability to reject unwanted measurements [36, 37]. Using the correlations between the state elements arising from the extrapolation of the **filter** covariance matrix, measurements of one state element can also provide improvements in its correlated elements. For example, a single navigation measurement of a spacecraft's position component can provide improved estimates in correlated spacecraft velocity components.

4.1.4 *Space Sextant*

The Space Sextant is an optical instrument that is used to sight simultaneously on stars and earth or planetary landmarks, measuring the angles between the lines of sight to these objects. In this manner the Space Sextant functioned like the astrolabe and sextant used by seafaring navigators [38]. Figure 6 shows a schematic of the Apollo Space Sextant. In the figure, the landmark line of sight (LOS) is fixed to **the** spacecraft and is pointed to a horizon or landmark by maneuvering the spacecraft. The star line of sight direction has two degrees of freedom: rotation about an axis parallel to the landmark LOS; and the second controlled by tilting the trunnion axis mirror. Measurements are made by superimposing the desired star and the landmark image lines of sight and recording the trunnion angle. The angle of tilt of the mirror, as in conventional sextant operation, is the desired measurement and is processed by the **Kalman** filter to update the current estimates of **the** vehicle state [39].

The Space Sextant is also used to maintain the alignment of the spacecraft Inertial Measurement Unit. Using the spacecraft computer to maneuver the vehicle to point the sextant at a known star, the offset of the star from the sextant boresight yields the necessary data to realign the IMU. This procedure is performed often enough so that the desired star is within the sextant field of view **even** in the presence of off-nominal IMU drifts.

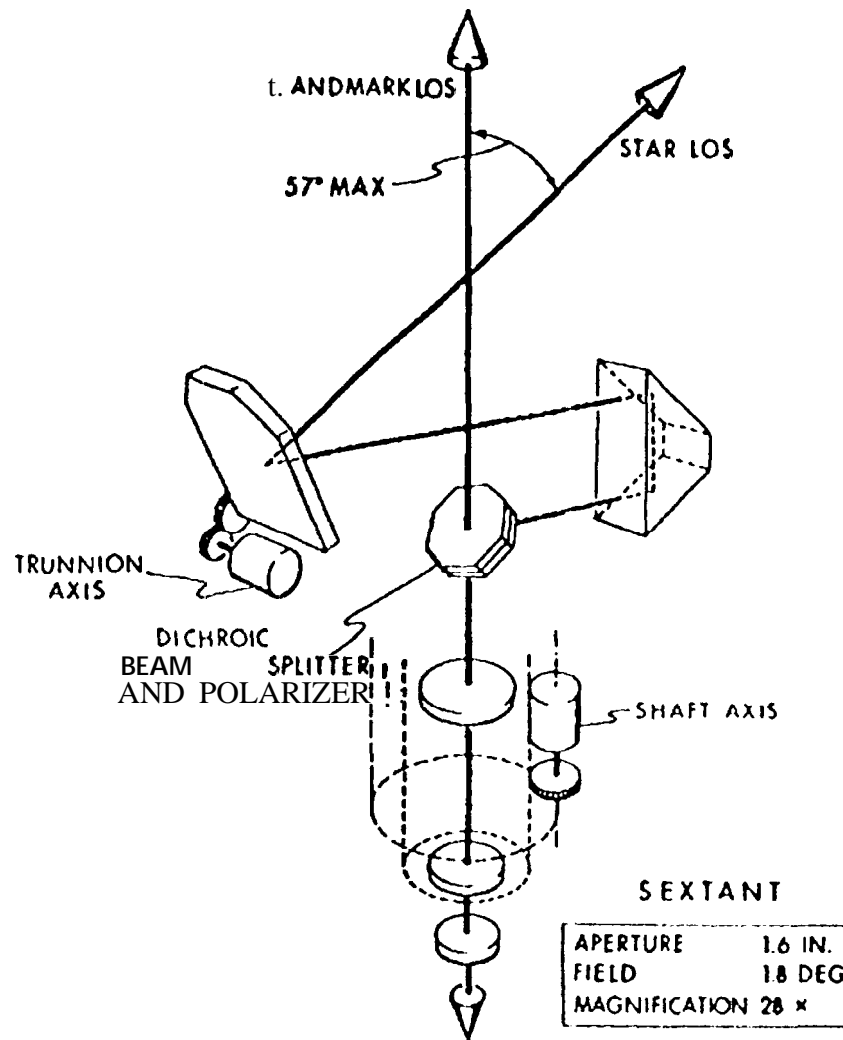


Figure 6. Apollo Space Sextant

4.2 Mission Phases

Missions are divided into phases or segments according to the objectives of a particular series of spacecraft operations. Table 1 lists representative manned mission phases applicable to manned space programs, the ground and on-board navigation sensors used and the designation of which system nominally provides the prime state estimate solution for that phase. Note that for the ascent, rendezvous and entry through landing mission phases, the on-board solution is prime.

The Apollo lunar landings contained mission phases applicable to all lunar and earth orbiting manned spacecraft operations. Figure 2 shows the Apollo mission profile and will be used for illustrative purposes in the following discussion of generic manned spacecraft mission phases. The ascent mission phase is initiated at vehicle liftoff from the earth or lunar surface, includes powered flight, coast and maneuver sequences, and terminates in a safe, stable spacecraft orbit about the attracting body. (Apollo contained two ascent mission phases, one from earth liftoff and the other from lunar liftoff). The orbit coast mission phase follows and is

Mission Phase	Ground Navigation Sensors	On-Board Navigation Sensors	Prime Navigation Solution	
			Ground	On-Board
Ascent	“ Manned Space Flight Network (MSFN) C-Band, S-Band Radars: Range and Doppler Measurements; LOS Angle Measurements from S-Band “ Deep Space Network Radars: Doppler Measurements	Command and Service Module (CSM) Inertial Measurement Unit: Velocity Change in 3 Axes of Inertial Frame		x
On-Orbit Coast		Space Sextant: Manual Star - Horizon Measurements	- x	
Trans - Lunar coast		Space Sextant: Manual Star-Horizon Measurements	X	
Lunar Orbit Coast		Space Sextant: Manual Known and Unknown Landmark Tracking	x	
Powered Descent		Landing Radar: Automatic Range and Doppler Measurements		x
Lunar Ascent		LEM Inertial Measurement Unit: Velocity Change in 3 Axes of Inertial Frame		x
Lunar Rendezvous		Lunar Excursion Module (LEM): Automatic Rendezvous Radar Transponder Tracking: Range, Range-Rate, LOS Angles and IMU Sensed Velocity Change During Maneuvers CSM: Manual Space Sextant Tracking of Blinking Light on LEM, Automatic VHF Ranging and IMU Sensed Velocity Change During Maneuvers		x
Trans-Earth coast		Space Sextant: Star - Horizon Measurements	x	
Entry		CSM Inertial Measurement Unit		x
Landing		CSM Inertial Measurement Unit		x

Table 1. Apollo Manned Mission Phases, Navigation Sensors Used, Prime Navigation Solution

defined as that phase during which the spacecraft orbits the attracting body. The orbit can be that resulting from the ascent phase or from different orbits achieved by the firing of its propulsion system. interactions with another spacecraft are not typically included during this mission phase. During a trans-earth or trans-lunar coast mission phase, the spacecraft is on a trajectory which

will take it from its original orbit to the vicinity of another ^t attracting body. (Figure 2 shows the **trans-lunar** and **trans-earth** coast phases of the Apollo missions.) During this phase the spacecraft is maintained on the desired trajectory by scheduled corrective maneuvers. As the spacecraft approaches the new attracting body, it can then be placed in orbit about this body using a series of maneuvers to attain the desired orbit and begin the orbit coast mission phase to support subsequent mission objectives. The landing phase normally **begins** with the descent initiation maneuver, or **deorbit** bum, which takes the spacecraft from its orbital coast condition and places it on a trajectory which will intercept the desired landing site. A powered descent such as was used in Apollo for the moon landings or an aerodynamic entry phase such as that used by the Shuttle then brings the spacecraft to a controlled landing on the surface. The landing phase may or may not be supported by external navigation aids and may rely completely on navigation sensors carried on board the spacecraft. For example, Apollo **lunar** landings relied on spacecraft inertial navigation, and landing radar range and Doppler measurements. Shuttle landings, [^] **however, are** supported by TACAN and Microwave Scanning Beam Landing System (MSBLS) stations located at the landing site. Another orbit phase is the rendezvous mission phase which consists of the tracking periods and maneuver sequences that are required to bring the chaser vehicle to docking condition or small stable relative offset with the target vehicle. This phase is distinct from the orbit coast phase and involves different navigation sensors, and in some cases, a different navigation system.

4.3 Role of **On-Board** and Ground Navigation

During all mission phases, the on-board and ground navigation systems are used simultaneously. Each system provides vehicle position and velocity estimates which are used for independent targeting of maneuvers to accomplish the objectives of that mission phase. The use of ground and on-board navigation capabilities, the navigation sensor data types employed, the computational and operational capabilities, and the primacy of either the on-board or ground solutions in providing the state estimates of the spacecraft, are dependent on the navigation accuracies that each can bring to a particular mission phase. When the ground provides the most accurate state estimates, these estimates are used to periodically reset the on-board state estimates so that maneuver **targeting** and execution can be performed using the on-board systems. In some cases, as was done for the precision Apollo 12 **lunar** landing, on-board navigation system measurements are used real time in conjunction with ground navigation observations to enhance the accuracy of the vehicle state estimate provided by the ground system. The improved accuracy ground solution then provides the on-board system with the accurate state estimate. **This** use of combined on-board and ground navigation system capabilities results in high accuracy, robust, and backup navigation capabilities for all mission phases. These combined capabilities have enabled the successful completion of nominal and more demanding enhanced mission objectives.

Table 2 shows the navigation system accuracy capabilities for typical manned mission applications. They are listed by mission type and mission phase. On-board solutions are prime if they are within **pre-mission** defined limits of the ground solution. Note that for the Apollo trans-earth and trans-lunar coast mission phases, the [Navigation capabilities are defined in terms of acceptable orbit condition errors, reentry angle error and **perilune** altitude estimation accuracy, respectively. For the rendezvous mission phase, the navigation tolerances are defined in terms of resultant midcourse maneuver targeting errors. These midcourse maneuvers maintain the active vehicle on an intercept trajectory with the target vehicle.

4.4 **Navigation** Coordinate Frames

The navigation coordinate frame chosen for both the ground and on-board determination of the spacecraft state, for trajectory prediction and for maneuver targeting, is a planet centered

Mission Phase	Apollo		Shuttle	
	Ground	On-Board	Ground	On-Board
Ascent	400 to 1000 ft; 3.0104.0 fps	400 to 1000 ft; 3.0 to 4.0 fps	200 ft, 1 "s	100 ft, 1.0 fps
Earth Orbit Coast	1000 't, 1 "s	Periodic Ground Uplink	3000 't, 3 "s	Periodic Ground Uplink
Earth Orbit Rendezvous Midcourse Correction Targeting Errors	1.5"s	0.3 "S	1.5 "S	0.3 "S
Trans-Lunar Coast • Perilune Altitude Estimation	68.8 nm	67.5 units?		
Lunar Orbit Coast	?	?		
Powered Descent	?	?		
Lunar Ascent Errors	?	?		
Lunar Rendezvous Midcourse Correction Targeting Errors	1.5 fps	0.3 fps		
Trans-Earth Coast • Entry Angle Estimation	-6.39 deg.*	-6.26 deg.*		
Entry: TACAN Acquisition			3000 ft, 3 fps	66000 ft, 60 fps
Landing		10s of nm	50	15 ft., 0.5 fps

● Actual values for Apollo 11

Table 2. Manned Mission Navigation Accuracies 1 σ)

inertial coordinate frame whose axes remain in a fixed direction relative to the celestial sphere. This frame is centered at the planetary body whose gravitational pull currently provides the dominant effect on the spacecraft motion. The directions of the coordinate frame axes are chosen relative to directions fixed with respect to the celestial sphere at a given epoch. For example, the Shuttle inertial frame is designated the Mean 1950 frame and is defined as follows: the x axis is toward the point of the vernal equinox, that is the point of intersection of the ecliptic (plane of the earth's orbit about the sun) and the earth's equatorial plane, where the sun crosses the equator from south to north. The z axis is normal to the ecliptic plane and they axis completes the right-handed system.

During missions where the gravitational force of more than one attracting body must be considered such as the Apollo trans-lunar or trans-earth coast phases, the center of the inertial coordinate frame changes to preserve the accuracy of the state vector propagation equations as the spacecraft leaves the vicinity of one attracting body and gets closer to the other body. The change in coordinate frames occurs when the spacecraft enters the sphere of influence of the attracting body whose gravitational field will subsequently provide the dominant effect on the spacecraft trajectory. The sphere of influence is defined as the roughly spherical surface centered on the attracting body, where the magnitude of two ratios, each ratio formed by dividing the disturbing acceleration due to one body by the gravitational acceleration due to the other body, are equal. In the Apollo program, the effect of the disturbing acceleration of the earth on the spacecraft trajectory when the spacecraft were within the lunar sphere of influence was ignored. Similarly, the gravitational effects of the moon were ignored when the spacecraft were within the earth's sphere of influence. For the Apollo program, the radius of the earth's sphere of influence is 49,579.2 nmi and the lunar sphere of influence radius is 35,714.9 nmi.

4.5 Ground Based Navigation

The ground-based navigation system consists of a network of tracking stations around the earth and a central facility, mission control, which processes the tracking data and communicates with the vehicle. The ground stations are located such that one or more stations can normally view the vehicle simultaneously. Depending on the mission phase and station capabilities, measurements of the spacecraft range and Doppler relative to these stations, as well as angle measurements of the line of sight from the station to the spacecraft, are made. The measurement data is transmitted to the **central** ground processing facility at mission control for determining the state of the spacecraft. The ground solution is then **uplinked** to the on-board system for use in resetting the on-board navigation state. These ground uplinks occur according to a set of **pre-mission** defined flight **rules**. The flight rules specify the maximum allowable difference between the on-board and ground state vectors which force a ground **uplink**, and they define which state estimate is prime for that mission phase.

4.5.1 Navigation Data Types and Their Information Content.

The ground navigation system utilizes **measurements** of the spacecraft range and velocity relative to the ground tracking stations, and, if available, angle measurements of the line of sight **to the spacecraft**. For earth orbit operations, C-Band skin track radars and S-Band stations, **which track** transponders on the spacecraft, are used. The S-band stations provide the full set of measurements. For lunar missions the Deep Space Network tracking facility is used and provides range and Doppler measurements to the spacecraft.

In the case when a measurement of the spacecraft speed relative to the ground station is made, the velocity data are known as two-way or three-way Doppler, depending on which station receives the signal. The data collected at the station that both sends and receives the signal are **called** two-way Doppler and the data collected at the station that only receives the signal are called three-way Doppler [40].

Apollo used the Manned Space Flight Network (MSFN) tracking stations which consisted of a net of stations located around the earth such that **a least three** stations could view the vehicle simultaneously except when the vehicle was in low earth orbit or behind the moon. The MSFN consisted of three 8 ft. and 11 30 ft. S-Band stations. These stations measured range and two-way and three-way Doppler [41].

4.5.2 Data Processing and System Operations

The vehicle state was determined in pre-Shuttle manned programs by ground navigation systems employing a **Bayesian** least-squares batch estimation technique to process the measurements from the ground-based radars. System model parameters were adjusted based on a comparison of the estimated Doppler and range measurements from the propagated vehicle state estimate with subsequent actual measurements from the ground tracking stations. The estimated vehicle **state** was propagated with high-order gravity and atmosphere models, as applicable. This estimation technique required manual assessment of the validity of the measurement residual (difference between estimated and measured values) to obtain the best orbit **fit**. It was a time and labor intensive process, resulting in a staleness of the state estimate. For **lunar** orbits, where the gravity mode] was not accurately known initially, the navigation process also included the modification of the gravity model using observed changes between the orbit ephemeris from the batch estimation programs and that observed from radiometric measurements [40].

Incorporation of a **Kalman filter** recursive state estimation **capability** significantly improved the estimation process. It eliminated the manual intervention required to assess measurement residuals and provided a **cent inuous** capability to incorporate measurement data as

it is acquired. In addition, the state estimated by the filter could be augmented to include gravity and other disturbing accelerations, in addition to the vehicle position and velocity. In this manner, an automatic adjustment of all estimation parameters can be made on a recursive basis.

Although the radar measurements are relative to ground stations fixed to the earth, the ground state estimate is obtained in the inertial coordinate frame discussed above and centered at the planetary body within the sphere of influence of which the vehicle is located.

4.5.3 Navigation Performance and Impact on Guidance

Ground state estimates cannot accurately account for the orbit perturbations arising from unscheduled spacecraft vents, crew-imparted spacecraft translation, and uncoupled translation effects due to spacecraft reaction control jet firings for attitude control. The most accurate ground solutions are obtained during a quiescent spacecraft tracking period in which no external disturbances other than the physical environment are placed on the vehicle. Once the solution is obtained, propagating this solution forward in time for uplink purposes degrades the accuracy of the solution, since spacecraft maneuvers are not accounted for in the propagation. The result is a reduction in the accuracy of the spacecraft state estimate and the resulting maneuvers targeted with the ground solution. The ground has normally targeted the following maneuvers, as applicable, for all manned programs: orbit change maneuvers, translunar and trans-earth maneuvers, and the deorbit maneuvers for landing. For the Space Shuttle program, the ground also targets the rendezvous phasing and height maneuvers to set up the appropriate Orbiter-Target vehicle relative position and velocity, prior to the initiation of the on-board relative sensor tracking.

4.6 On-Board Navigation Systems

On-board navigation systems contain the appropriate sensor configurations and estimation algorithms to maintain an estimate of the spacecraft position and velocity independent of the ground. The on-board system uses the same inertial reference frame as the ground. As discussed above, the frame is centered at the planetary body whose gravitational pull provides the dominant effect on the spacecraft at its present location.

To determine the spacecraft trajectory for orbital coast, coasting flight between planetary bodies, planetary landings and for rendezvous with a target vehicle, on-board systems use navigation sensors which define components of the spacecraft state relative to this inertial frame. Measurement data from several different sources are used in each mission phase, to provide spacecraft range, range rate and line-of-sight direction information to known or unknown external sources. These external sources can be other planetary bodies, target spacecraft, or physical phenomena associated with a planet, such as landmarks and horizons.

4.6.1 Navigation Data Types and Their Information Content

4.6.1.1 Inertial Measurement Unit

The inertial measurement unit is probably the key navigation sensor on the spacecraft. By aligning its axes in a known orientation relative to the celestial sphere, and knowing the alignment of the inertial navigation frame in the celestial sphere, the alignment between the inertial unit and the inertial navigation frame is also known. Since the coordinate transformation between the inertial unit platform axes and the vehicle body axes is also known (determined when the inertial unit is mounted on the vehicle), the attitude of the vehicle and the linear motion of the spacecraft arising from propulsion system maneuvers or from atmospheric forces is measured by the gyroscopes and accelerometers respectively.

4.6.1.2 *Doppler and Range*

The spacecraft can determine its orbit relative to a **planetary** body or a landing site during planetary landings, by measuring its range and range-rate (Doppler) relative to the surface, to ground stations at known locations on the planetary surface or to satellites whose positions and ephemeris are accurately known. By processing **these** measurements sequentially in the on-board **Kalman filter**, the on-board system can determine the spacecraft trajectory.

Range and range-rate measurements are also used during the rendezvous **mission** phase. Without angle measurements of the line of sight to the target vehicle, they can provide information about the relative trajectory which, for some trajectory conditions, is inadequate to place the chaser vehicle on a **trajectory** to intercept the target. For other trajectories, range and range-rate measurements by themselves cannot accomplish rendezvous. Using range, range-rate and line-of-sight measurements to the target, the complete relative state and trajectory of the **chaser** vehicle with respect to the target can be precisely determined to achieve accurate target intercept.

4.6.1.3 *Optical Navigation*

Optical navigation techniques are used for accurately determining the spacecraft trajectory during orbit coast about the planetary body and during coasting flight between planetary bodies. Optical measurements of planetary diameters, of the angle between a star and the planetary sub-stellar horizon point or planet center, of the angle between two stars, and of the planetary horizons, can be used to accurately determine the spacecraft trajectory. These measurements can either determine a line-of-sight direction which, through the use of the IMU, is referenced to the inertial navigation frame, or they can determine the angle between planetary and stellar phenomena which is dependent on the current spacecraft position. Processing these measurements recursively in the on-board **Kalman filter** determines the spacecraft position, velocity and trajectory in the inertial frame.

Precision landings of a spacecraft relative to a designated landing site can be achieved by the optical tracking of known or unknown planetary landmarks or distinguishable surface features which are at known locations relative to the desired landing site. These measurements define the location of the landing site relative to the spacecraft trajectory in the inertial navigation frame. This technique effectively eliminates map errors, referencing the accurate relative locations of features from surface maps to the inertial reference frame [44].

For rendezvous applications, measuring the direction of the line of sight to the target and referencing this direction to the inertial navigation frame can provide, by itself, an estimate of the relative state between the chaser and target vehicles. Over time, using the geometry change between the vehicles due to orbital mechanics, and the correlations developed in the **Kalman** filter by propagating the covariance matrix, the complete relative state is determined such that accurate targeting of the required maneuvers to effect rendezvous is accomplished. Since the range to the target is not accurately known with only optical measurements, however, the time of arrival at the target can vary from the desired intercept time.

4.6.1.4 *Data Processing and Estimation Techniques*

An extended **Kalman** filter formulation has been used to sequentially process on-board navigation measurements for **Apollo** and all subsequent manned programs. The filter state size is dependent on the sensors being used, measurement error sources being accounted for, and disturbing accelerations being estimated. In the extended **Kalman** filter formulation, both the propagation and measurement equations are linearized about the current estimated trajectory, thus maintaining the necessary filter linearity.

The **Kalman** filter formulation requires that the **covariance** matrix, which reflects the statistics of the accuracy of the state estimates, remain symmetric and positive-definite. For navigation applications where the computer does not have enough accuracy to maintain this symmetric positive-definite condition after processing many measurements, a "square-root" **Kalman** filter formulation is used [35, 44,45, 46]. If the computer has the requisite accuracy, the full **covariance** matrix formulation can be used. This results in improved filter capabilities and reduced manual operations.

The position and velocity estimates, and the filter **covariance** matrix, are propagated along the current estimated trajectory, using on-board drag and gravity models, as required, with the model **fidelity** appropriate to the accuracy requirements for the given mission phase. Accelerometer measurements of the vehicle translation from propulsion system firings or atmospheric drag **are** also used in the propagation equations, with the attitude of the vehicle determined from the inertial measurement unit gyroscopes.

4.7₀ Degree of Manual/Automatic Operations

On-board navigation system operations are controlled by the crew. Selection of the appropriate navigation programs for execution in the on-board computers and the monitoring of hardware and system performance are crew functions. Manual involvement in measurement taking and measurement processing has been reduced with each succeeding manned program. The recursive navigation capabilities of the **Kalman** filter, the capability for measurement editing inherent in the algorithm and the increased capabilities and accuracies of digital computers have enabled a marked reduction in required manual operations and a marked increase in navigation capabilities. This will be made evident in the discussions of the Apollo and Shuttle on-board navigation system operations that follow.

4.8 Apollo Lunar Landing Program

The Apollo Lunar Landing Program was highly successful, resulting in six manned landings on the moon. Both ground and on-board navigation systems were used during all mission phases as planned. The navigation solutions from each **system** complemented each other in providing highly **accurate** state estimates for **all** mission phases, resulting in the successful accomplishment of all mission objectives. The rendezvous, **orbit** coast and descent navigation systems were checked out in a **series** of two **earth-orbital** missions and two lunar missions before the Apollo 11 **lunar landing**. The **critical** rendezvous navigation systems of the Lunar Excursion **Module (LEM)** and the Command and **Service Module (CSM)** were tested in three of the four flights.

4.8.1 *Ground Navigation*

Ground navigation for the **Apollo** program was performed using the Spacecraft Tracking and Data Network (**STDN**) ground stations: three 85-foot and eleven 30-foot S-Band stations. These stations measured range and both two-way and three-way Doppler to the spacecraft. The data was transmitted to the Mission Control Center for processing in the MCC computers.

A batch processing technique was used to process the measurements and to determine the **vehicle** position and velocity. During Apollo 8, **10** and 11, the **lunar** gravity model used in the ground navigation program was found to be not accurate enough to predict the spacecraft orbit ahead for any appreciable length of **t i me**. Over the course of each mission, the model was continuously updated based on **manual** observations of the discrepancy between the predicted orbit and the actual measured orbit. Addition of mass concentrations to the lunar gravity model

eventually produced a gravity model which fit the predicted orbit with the actual measured orbit. The ground state vector was then transmitted to the Command Module as defined by flight procedures, either prior to major events or when ground and on-board state comparisons exceeded **pre-mission** defined tolerances [40,41, 44].

4.8.2 *On-Board Navigation, Ground/On-Board Operations and Mission Phases*

4.8.2.1 *Apollo Guidance Computer*

The Apollo Guidance Computer (**AGC**) was a fixed-point ones complement real-time digital computer. It contained 36,864 words of read-only memory and 2,048 words of read/write memory and had a cycle time of 12 microseconds. Each word in memory was 16 bits, and data words were signed 14 bit words. Communications between the **AGC** and the crew were through the display and keyboard, which enabled the astronauts to transmit commands (verbs) and requests (nouns) using a vocabulary of 99 nouns and 99 verbs. The computer software operated as a real-time multiprogram system, sharing the CPU to accomplish all tasks required during a given mission phase [35, 42, 43].

The computer had a large library of routines that performed higher-level mathematical and language operations, thus trading off execution speed against economies in programming the necessary algorithms. A high density read-only memory, called a rope memory, was developed. This type of memory was used because of its high density and reliability. It can be altered only by re-manufacture, repair or destruction [35].

There was a single AGC on each spacecraft. No in flight computer hardware failures occurred. Such near perfect reliability was achieved with attention to design, the constraint of a minimum number of different parts, detailed engineering and qualification of design and components, and 100 percent stress testing of the parts to be used in manufacture [42].

4.8.2.2 *Apollo Inertial Measurement Unit*

The Apollo Inertial Measurement Unit was a derivative of that used for the Polaris missile guidance system. The Apollo mechanism was simplified from the Polaris unit by providing only three degrees of freedom in the gimbals. A stellar alignment capability was also added to the Polaris inertial unit. Use of three gimbals instead of four also enabled a higher accuracy in alignment of the unit with the optical star sightings. No IMU failures occurred in over 2500 hours of in-flight operations. The IMU was aligned using the Space Sextant discussed above by determining the angle offset between the actual and estimated star positions in the Sextant field of view [35, 42].

4.8.2.3 *Recursive Navigation Kalman Filter*

The CSM and LM navigation systems used an extended Kalman filter formulation with the filter state size dependent on the mission phase. To maintain positive-definiteness of the filter covariance matrix after a large number of operations using the small word-size computer, the filter used the square-root formulation of the covariance matrix. This formulation also reduced computational requirements. Process noise was not used to keep the filter active due to the computational complexity of using process noise in a square-root formulation. In favor of computational simplicity, periodic manual reinitialization of the square root matrix, at pre-mission determined times, enabled the continuous incorporation of measurements [44, 45]. The same Kalman filter algorithm, or structure, was used for processing the navigation sensor measurements for all mission phases. Figure 7 is a simplified diagram of the Apollo recursive navigation concept.

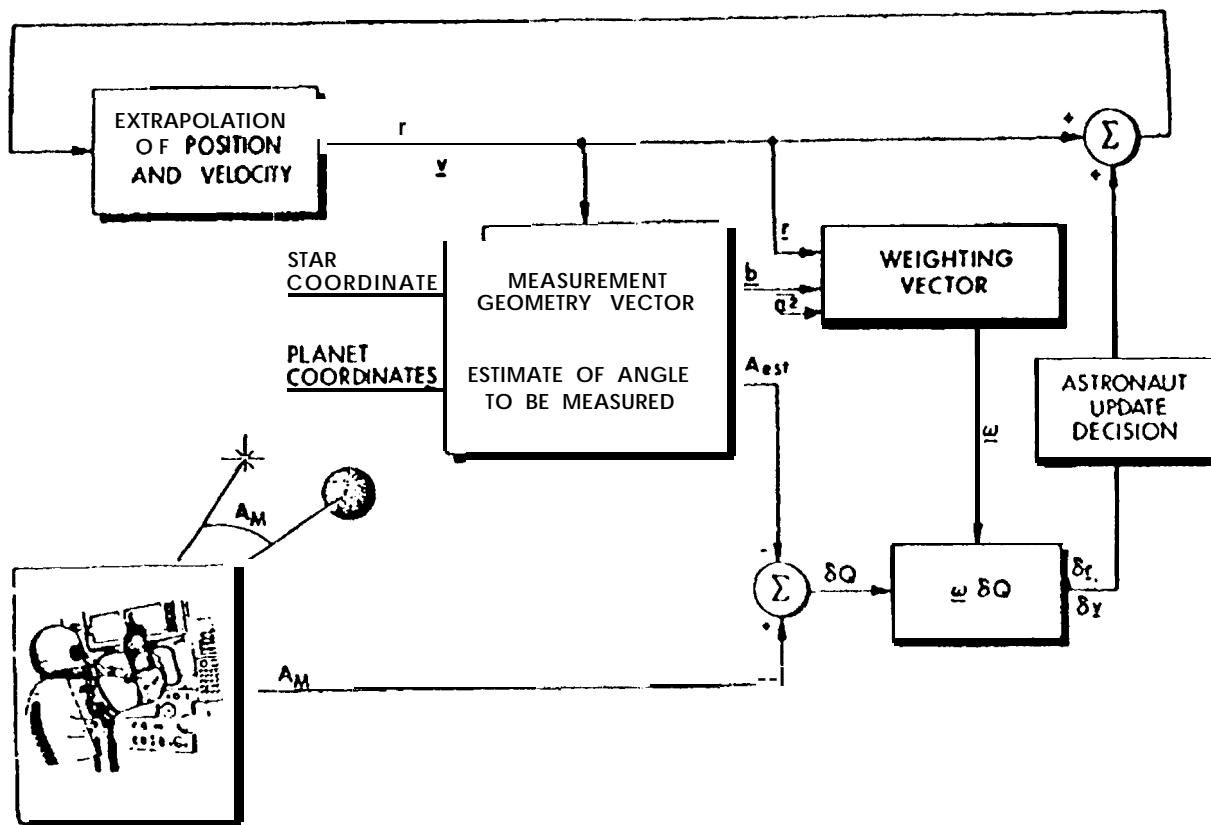


Figure 7. Simplified Apollo Recursive Navigation Functional Diagram

4.8.2.4 On-Board Navigation and Ground /On-Board Operations

The Command and Service Module navigation sensors shown in Figure 8, and the Lunar Excursion Module sensors shown in Figure 9, were used to provide estimates of the spacecraft state. Depending on the mission phase, the on-board or ground solutions were used as the prime state estimates. Pre-mission developed operational procedures were defined to provide the most effective use of both the on-board and ground navigation capabilities for each mission phase.

During earth orbit coast, lunar orbit coast, and for the trans-lunar and trans-earth mission phases, on-board navigation was performed using the Command Module 28-power sextant to measure the angles between selected stars and the earth or lunar horizons. These measurements with a 10-arcsecond accuracy were used in the recursive Kalman filter in the CSM AGC. Calibration measurements of the Earth horizon bias were made during trans-earth coast to update horizon bias estimates in the navigation filter [46].

During lunar-orbit operations, surface landmarks were tracked by the CSM Scanning Telescope, a unity-powered instrument which measured the angle between the stellar aligned inertial unit and the line of sight to the surface feature being tracked [46, 47, 48].

For earth-orbit and lunar-orbit operation?, as well as trans-lunar and tram-earth coast, the ground navigation solution was prime. The on-board state estimates were used as backup solutions and, in the event of loss of communication with the ground, had the required accuracy to target and execute maneuvers for the safe entry and landing of the crew.

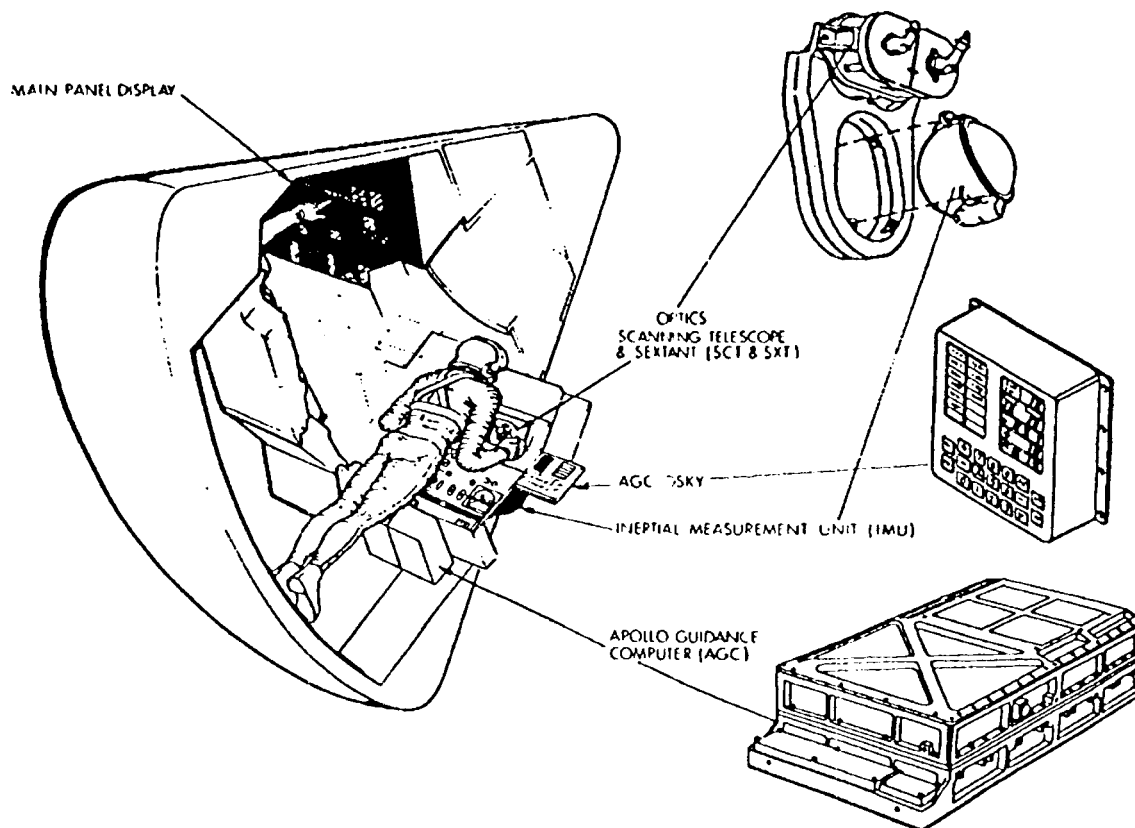


Figure 8. Apollo Command and Service Module Navigation Sensors

The navigation state estimates were used to compute velocity corrections to keep the spacecraft on the proper trajectory to and from the moon.

During the lunar-orbit rendezvous, both the CSM and the LM performed rendezvous navigation. Both systems targeted the rendezvous maneuvers for comparison of solutions and for a CSM backup capability for rescue in the event the LM was not able to execute the maneuver. The ground also tracked both vehicles and computed the rendezvous maneuvers. Based on pre-mission analysis and the setting of maneuver comparison limits between all three solutions, the LM, CSM and ground solutions were prime, in that order. Since most of the rendezvous maneuvers were behind the moon, ground support was limited [43, 44, 45].

In the CSM, the crew used the Sextant to manually track a blinking light on the LM. This light could be seen at a distance of several hundred miles. The Sextant measured the direction of the line of sight from the CSM to the LM relative to the IMU. Marks were taken at the rate of one a minute. This line-of-sight information was processed in the Kalman filter as two angle measurements. Range measurements were made using the VHF communication link.

The LM used measurements from the rendezvous radar of the range, range rate and line-of-sight angles between the CSM and the LM. The rendezvous radar was an amplitude-comparison monopulse tracking radar which tracked a transponder on the CSM, providing a measurement set to the Kalman filter every minute. The tracking range was 300 nautical miles.

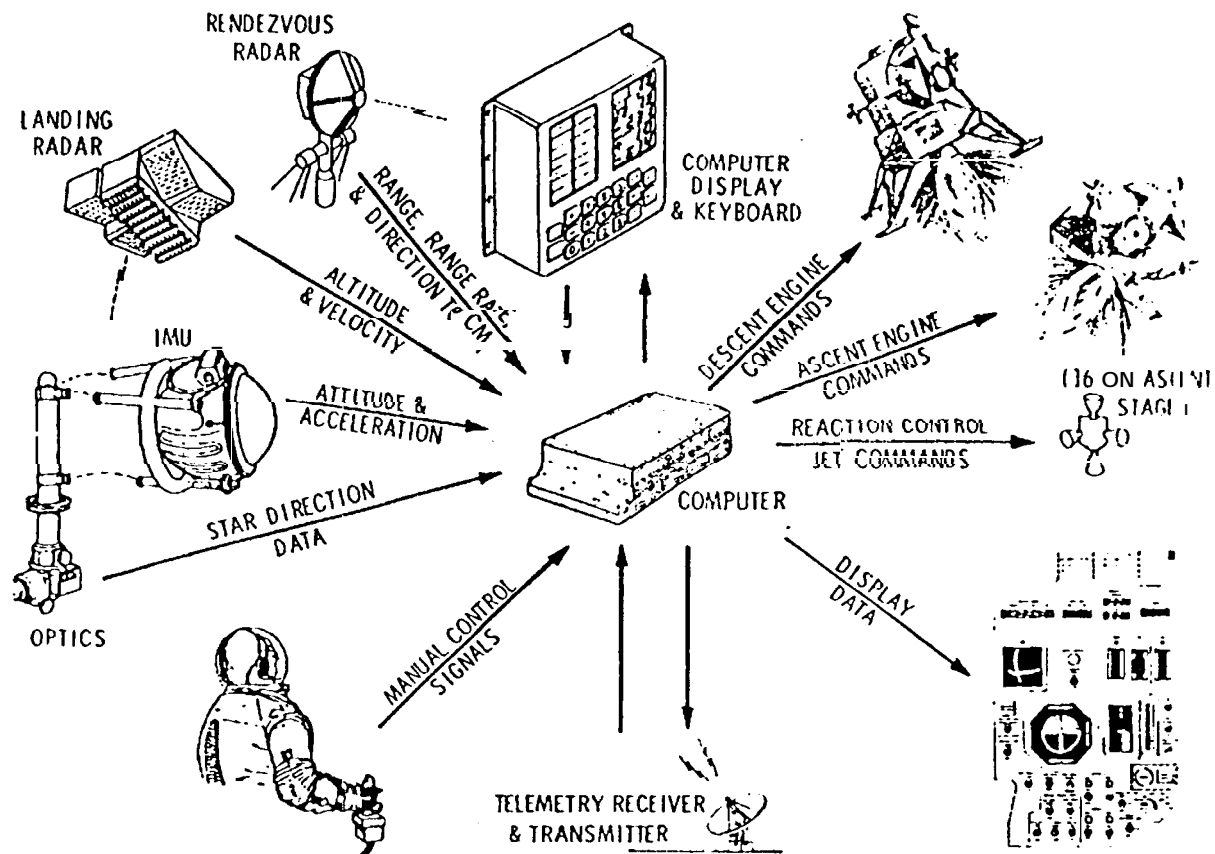


Figure 9. Apollo Lunar Excursion Module Navigation Sensors

In both the CSM and LM rendezvous navigation systems, the rejection of data which exceeded residual edit criteria and the periodic reinitialization of the filter covariance square-root matrix were manual procedures.

The rendezvous Kalman filter formulation in both vehicles assumed that the state of one vehicle was known perfectly. The filter updated the inertial state of the active vehicle relative to the "perfectly known" inertial target state [45].

A manual backup navigation technique was also provided. Angle data from visual observations of the local vertical angle of the CSM relative to the LM using the attitude direction indicator were plotted. These angles and their corresponding rate histories were tabulated during the coelliptic orbit (constant altitude difference) phase approaching the Terminal Phase Initiation maneuver. This data was used to calculate the coelliptic altitude difference between the CSM and LEM. This provided the velocity change required to initiate the terminal phase intercept maneuver in the event of a computer failure and communication failure. The rendezvous trajectory was designed so that this terminal phase maneuver was executed in the direction of the line of sight to the target. Pre-mission analysis determined the expected accuracies of all systems and the flight rules which governed the compare limits between these solutions to confirm the use of the AGC solution as prime [45, 48].

Powered lunar descent and landing used sensed **acceleration** as measured by the **IMU** to propagate the on-board state estimate. The landing radar, activated during the braking phase, provided altitude and velocity measurements relative to the surface. A filter implementation using scheduled gains, along with a terrain model for calculating estimated measurement parameters, was used to process these measurements for improving the vehicle state estimates.

For the Apollo 12 pinpoint landing near the Surveyor spacecraft, measurement data from CSM Sextant tracking of the landing site was **used** to tie the CSM orbit plane to the landing site. This data was used in the ground processor to update the location of the landing site by relating the **ground-determined** CSM orbit plane to the site using the Sextant data. (See section 4.6.1.3). The ground computed the delta position correction for the LEM and this was used to reset the **on-board** navigation prior to initiation of the powered descent.

Earth reentry navigation utilized the IMU for measuring sensed acceleration to propagate the state and compute the necessary roll commands to prevent skipping out of the atmosphere or too steep an entry which would cause heat and structural load limits to be exceeded. The IMU was also used to provide a drag altitude measurement for stabilizing the altitude channel [49].

This use of combined ground and on-board CSM and LEM navigation systems provided the Apollo program with a highly accurate, robust and redundant navigation capability which provided pinpoint lunar landings, successful lunar rendezvous and accurate entry and landing performance.

4.9 Skylab and **Apollo-Soyuz**

The **Skylab** program involved three extended-duration missions in an orbiting “Space Station” called Skylab. Skylab was the third stage of the Saturn V booster outfitted with laboratory, living quarters, a space telescope and a docking adapter for the crew delivery vehicle. The crew delivery vehicle was the Apollo Command and Service Module.

The Skylab missions employed the same combination of ground-based and on-board navigation system capabilities as was used for the Apollo Lunar Landing Program. The Manned Space Flight Network provided navigation during the orbital coast periods, for state updates to the CSM prior to the start of the rendezvous phase and state updates prior to the **deorbit** burn for returning the crew to **Earth**. In addition the ground updated the Skylab state vector during the crew **stay**.

On-board navigation during the CSM rendezvous with Skylab used the same techniques and navigation sensor measurements as the Apollo CSM rendezvous with the **LEM**. This consisted of the CSM tracking a flashing beacon on the Skylab and processing the measurements in the recursive navigation extended **Kalman** filter. The primary change in the computer for the earth-orbital missions was the scale factor used in the fixed-scale Apollo Guidance Computer. The scale factor was changed from that used in the lunar missions to reflect the low-earth orbit operations of the Skylab program.

During Apollo, as discussed above, both the **LEM** and CSM simultaneously performed rendezvous navigation, which resulted in both providing maneuver solutions for the rendezvous. **In** this manner a prime and a backup solution were always available, and in fact both solutions provided checks on each other. For the Skylab program, the second solution was provided by implementing a set of targeting algorithms on magnetic cards fed into a hand-held calculator. Inputs to **the** targeting algorithms were the data from visual observations of local vertical angle rate histories during the coelliptic orbit phase approaching the Terminal Phase Intercept Initiation maneuver. The visual data was recorded and input to the calculator to obtain solutions which

were compared to the Apollo Guidance Computer and ground solutions. Pre-mission analysis determined the **expected** accuracies of **all** systems and the flight rules which governed the compare limits **between** these solutions to confirm the use of the **AGC** solution as prime.

The **Apollo-Soyuz** program was the **first** rendezvous and clocking between spacecraft of two countries. This program involved **extensive** cooperation and coordination between the launch and ground operations of the U.S. and Russia. The Russian **Soyuz** was launched and placed in orbit before the launch of the **U.S. CSM** spacecraft. Russian ground-based navigation provided the state vector of the **Soyuz** prior to the **start** of the rendezvous mission phase. The CSM state at this time was provided by U.S. ground tracking. During the rendezvous, the **on-board** CSM performed optical tracking of the **Soyuz** to provide the **Soyuz** and CSM states for targeting the rendezvous maneuvers. The hand-held calculator was also used to provide backup solutions as was done for the Skylab rendezvous.

For both the Skylab and **Apollo-Soyuz** programs, the CSM entry navigation was the same as used for **Apollo**, relying on IMU data and pseudo-drag altitude measurements to contain the navigation state altitude error.

4.10 Space Shuttle Program

The initial designs of the ground and on-board navigation systems for the Space Shuttle program evolved from their respective systems in the Apollo program during the early 1970s. Figure 10 shows the Shuttle mission profile and the associated mission phases: ascent/aborts, on-orbit operations, rendezvous, and entry through landing. As in the **Apollo** program, ground and on-board navigation capabilities and solution accuracies are a function of mission phase.

LEGEND

MECO = MAIN ENGINE CUTOFF

OMS = ORBITAL MANEUVERING SYSTEM

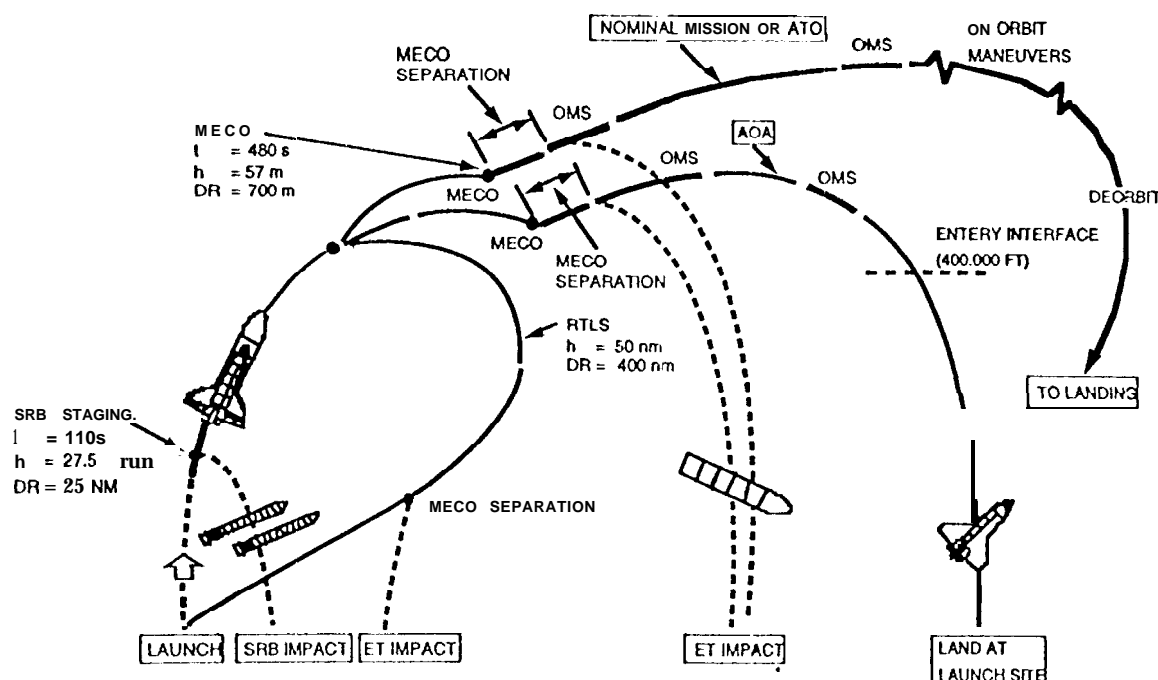


Figure 10. Shuttle Mission Profile

The ascent phase begins at liftoff with the Solid Rocket booster and three main engine powered **flight portions** of the flight. **If no abort** is declared, the powered flight phase is followed by one or two On-orbit Maneuvering System (OMS) burns which place the Orbiter in a **circular** orbit about **the Earth**. If an abort has been declared during the ascent powered flight phase, the Orbiter is placed on a trajectory consistent with the abort profile, either a Transatlantic Abort, Return to Launch Site, Abort to Orbit, or Abort Once Around. If no abort is declared, On-orbit operations **are** initiated. **If** rendezvous with a target vehicle is required, the rendezvous mission phase is initiated and it terminates with the grapple of or docking with the target vehicle. The Entry mission **phase** begins shortly before **the deorbit** burn which takes the Orbiter out of orbit and places it on the entry trajectory. The orbiter enters **the** atmosphere at 400,000 ft at a 40 degree angle of attack and performs a series of S-turns to control the downrange and **cross-track** trajectory to the landing site.

4.10.1 *Ground Navigation*

The Shuttle ground navigation system uses range and Doppler measurements, and measurements of **the** spacecraft line of sight from C-Band and S-Band tracking stations. Air Force Eastern Test Range radars are used during ascent, and the Manned Space Flight Network stations are used for the on-orbit, rendezvous and entry phases. With the launch of the Tracking Data and Relay **Satellite System (TDRSS)** satellites in the 1980s, tracking of the Orbiter with two-way ranging through **TDRSS**, using the orbiter Ku-band radar and ground stations at White Sands, provides an enhanced ground navigation capability which reduces the time to obtain an Orbiter navigation **fix**. Two twenty-minute **TDRSS** tracking passes over the course of an orbit is all that is currently required to provide accurate ground-based estimates of the Orbiter state. During ascent, orbit and entry operations, ground C-Band and S-band radar and TDRSS tracking of the Shuttle, are used to provide measurements for the Mission Control Center High Speed Navigation Determination processor [50]. This processor uses an extended **Kalman** filter recursive navigation formulation for processing the measurements.

The ground state **estimates** are used to reset the on-board Orbiter state when the on-board and ground states differ by **pre-mission** defined values. These ground **uplinks** can occur after the ascent powered **flight** phase, at the start of the entry phase, periodically for resetting of the **on-board** state during orbital coast, and for providing the Orbiter and Target vehicle states at the start of the rendezvous mission phase.

4.10.2 *On-Board Navigation and Ground/On-Board System Operations and Interdependency*

The on-board navigation system techniques and capabilities are mission phase dependent. The sensors used are illustrated in Figure 11, Table 3 lists the navigation applications and navigation sensors used for each Shuttle mission phase. A redundant set of on-board flight computers is used to provide a fail-operational, fail-safe capability.

4.10.2.1 *Shuttle General Purpose Computers (GPCs)*

The Shuttle carries five General **Purpose Computers (GPCs)**. Three are used by the Primary Avionics System, **one** for system management and the other for the Backup Flight **S**ystem. The GPCs are floating-point **IBM AP101 S** computers with 256K memory. The floating-point word length is 32 bits. **These** computers provided a substantial increase in capability from the Apollo Guidance Computer.

One **of** the benefits of the increased word length to the on-board Shuttle navigation system development was the use of the **full covariance matrix** formulation in the rendezvous and entry **extended Kalman** filter formulations. This formulation, coupled with the increased

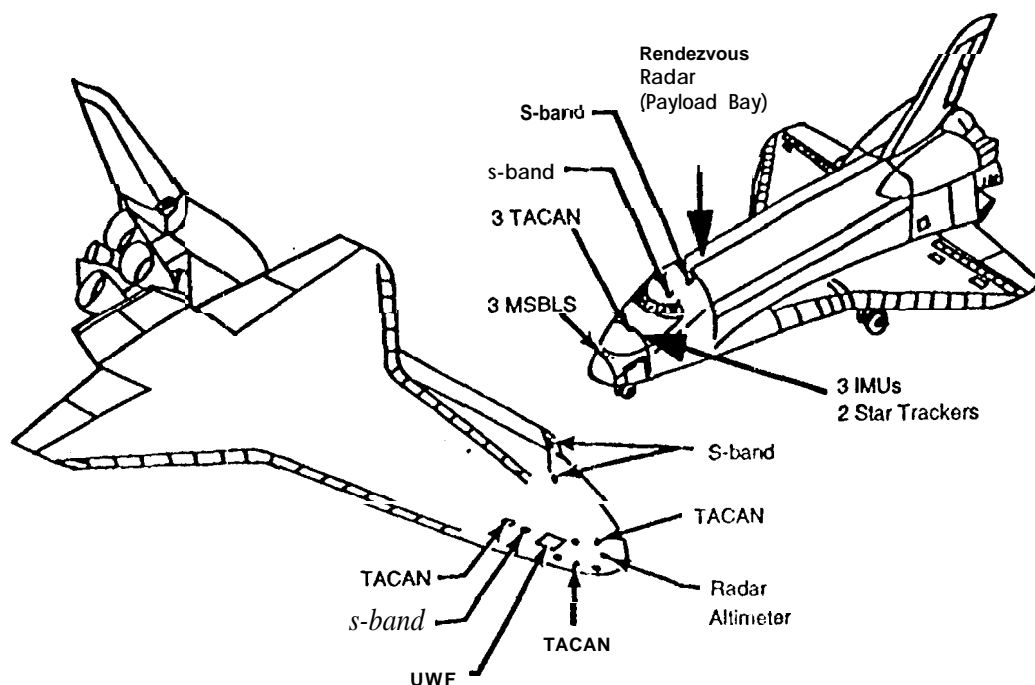


Figure 11. Shuttle Navigation Sensors

Mission Phase	Ground Navigation Sensors	On-Board Navigation Sensors	Prime Navigation Solution	
			Ground	On-Board
Ascent	Eastern Test Range C-Band and S-Band Radar Tracking: Range, Doppler and LOS Angle	Triply Redundant Inertial Measurement Units: Velocity Change in 3 Axes of Inertial Frame		X
On-Orbit Coast	Tracking and Data Relay Satellite System: Two-way Range and Doppler	Periodic Resetting of On-Board State to Ground Navigation State	X	
Rendezvous	MSFN C-Band Radar Tracking and TDRSS Tracking	Automatic Rendezvous Radar Skin Tracking: Range, Range-Rate, LOS Angles IMU Sensed Velocity Change Automatic Star Tracker Tracking of Target in Reflected Sunlight		X
Entry through Landing		Triply Redundant Inertial Measurement Units: Velocity Change in 3 Axes of Inertial Frame Pseudo Drag Altitude Measurements TACAN Range and Bearing ADTA Altitude Measurements MSBLS Range, Azimuth and Elevation Measurements		X

Table 3. Shuttle Navigation System Configurations

in the **M50** inertial coordinate system using the selected total sensed velocity change from the **triply** redundant **skewed** alignment Inertial Measurement Units. The navigation system maintains an estimate of position and velocity of the Shuttle **navbase** on which the IMUS are mounted. During the coasting portions of this phase, a 4x4 gravity model and a **Bab-Mueller** atmosphere model ~~are used~~ ^{are} to propagate the state.

For the on-orbit coast ~~mission~~ ^{are} phase, a 4x4 gravity model and a **Bab-Mueller** atmosphere model (which uses Orbiter **attitude**) are used in the propagation equations to maintain the current state estimate. Unlike the ~~Ascent~~ mission phase, the on-orbit navigation system maintains an estimate of the Orbiter **center of mass**. For thrusting periods, the redundant inertial measurement units are again used to provide a selected set of velocity counts for state propagation. Sensed velocity from the **IMUs**, which are located at the **navbase**, are corrected to provide the sensed acceleration at the center of mass. Ground navigation provides periodic updates to the on-board computer position and velocity, according to pre-mission flight rules which define difference limits between the ground and cm-board states. The Inertial Measurement Units are periodically aligned with star sightings from the two star trackers which are mounted on the navigation base. Two stars separated by roughly 90 degrees are used as are stars of opportunity during coasting periods. Unlike the Apollo sextant which required astronaut confirmation of the star in the sextant **field** of view, the Orbiter star trackers automatically identify the stars in their fields of view using the on-board state estimates and the star locations from the GPC star **table**.

Rendezvous operations are ~~initiated~~ ^{are} by aligning the IMU and setting the on-board Orbiter and Target states to the states ~~provided~~ ^{are} by ground navigation. The ground also provides maneuver solutions for the **height**-adjust and phasing maneuvers which place the Orbiter on a trajectory to intercept a stable orbit point eight miles behind the target. As the Orbiter closes on the target, optical measurements of the line of sight to the target are automatically taken by one of the two star trackers during the periods of reflected sunlight. These measurements are processed in the rendezvous **Kalman filter** as discussed above at a rate of one every eight seconds. Confirmation of optical target track is made by the crew using displays of the rendezvous navigation **Kalman** filter measurement residuals. The system is in "Inhibit" prior to the crew's enabling the automatic measurement **taking** and incorporation [53].

When the target is within the skin-track capability of the rendezvous radar, nominally 26 nmi, radar measurements of the range, range rate and line-of-sight angles of the target with respect to the Orbiter are processed by the rendezvous Kalman filter every eight seconds. The rendezvous radar provides measurements down to a target range of 100 ft. Manual control of the trajectory is initiated following the last midcourse ~~correction~~ at a range of 4000 ft. In the event of radar failure, the Orbiter star trackers can be used until eight minutes before the second midcourse correction (when the target enters darkness). The use of angle navigation alone accurately places the vehicle on an intercept trajectory.

The crew can also use navigation measurements made using the Crew Optical Alignment Sight, an instrument mounted in either the forward or overhead windows. This instrument is also used to confirm stars in the star tracker field of view, and for IMU alignment.

The **entry** mission phase is initiated by ground uplink of the Orbiter state to the on-board GPCs. Three on-board state estimates are separately maintained by the on-board system, each state associated with a dedicated IMU. Using **Bab-Mueller** atmosphere and 4x4 gravity models, as well as the **dedicated** IMU sensed velocity during the deorbit burn, the three states are propagated to entry interface. When the drag acceleration on the Orbiter is above the IMU **quantization level**, the IMU sensed acceleration (drag) and gravity model arc used to propagate the state. When the drag acceleration reaches 11 fps squared, drag altitude measurements are processed. These measurements are obtained by using the sensed acceleration to compute atmospheric density (using the standard drag equation) and using this density in the on-board

atmosphere model to compute an estimated altitude. The measured altitude is obtained **from** the navigation state. **These** drag altitude **measurements** prevent the altitude channel from diverging before external **navaid** measurements are obtained. Prior to the start of drag measurement incorporation the ground can, if necessary, perform an incremental delta state update (rather than the normal whole vector update) which effectively moves the Orbiter forward or backward **along** the trajectory while not changing the vehicle time tag.

Triply redundant TACAN receivers automatically provide range and bearing measurements to **the** GPCS for processing. Redundancy management software selects which of the measurements is to be used to update the three separate entry state estimates being maintained by the on-board navigation system, one for each of the three inertial measurement units. A state is selected for use in guidance calculations from the redundant navigation state estimates using a **mid,value** selection for each state vector component for the no **IMU** failure case.

When MSBLS is acquired, **triply** redundant MSBLS receivers provide re,dundancy management selected range, azimuth and elevation measurement for use by the single Orbiter state now being maintained by the navigation **system**. The MSBLS navigation capability provides state accuracy to support an autoland capability.

SECTION 5. FUTURE DEVELOPMENTS

What possibilities does **the** future hold for robotic and manned space navigation applications? For low earth orbiting missions and for **trans-lunar** and **trans-earth** trajectories, **extensive** use of operational GPS navigation systems will be routine. Feasibility studies have led to space borne GPS developmental test flights on the Space Shuttle and on unmanned NASA and DOD military satellites. **These** GPS systems will become operational and will provide, not only spacecraft position and velocity, but spacecraft attitude as **well**. The U.S. ~~Space Shuttle~~ ^{Space Shuttle} will be provided an integrated GPS navigation capability for all mission phases. ~~The International Space Station Alpha~~ ^{The International Space Station Alpha} will use GPS for position, velocity and attitude [52, 53,54, 55].

Advances in the miniaturization of electronic components **will** lead to lower-weight, lower-power, and higher-capability sensors and computer systems. Navigation sensors such as star trackers, rendezvous radars and landing radars will contain embedded processors capable of providing distributed, and **reconfigurable**, fault-tolerant systems. Micromechanical inertial measurement units will be combined with GPS to provide low cost, accurate navigation capabilities for the large number of communication satellites envisioned for **@global** wireless communications networks [56, 57].

Distributed computer architectures, **coupled** with advances in fault-tolerant **reconfigurable** computer systems and expert systems, will provide long duration fault-tolerant navigation operations. This **will** pave the way for autonomous (no human presence) and automatic (**enhanced** manual) operations for long duration lunar and interplanetary missions.

Development and deployment of Lunar and Mars radiometric navigation infrastructures similar to the that of GPS satellites and ground pseudo-satellites for earth orbit navigation **will** provide navigation for routine mission operations and precision landings similar to that on Earth [58].

Teleoperations and **telepresence** may be used for navigating rovers on the lunar and Martian surfaces. Automatic rovers will use the GPS - like navigation infrastructures for surface navigation.

Navigation systems will encompass expert system capabilities and artificial intelligence

for hardware and software system monitoring and reconfiguration and will be able to autonomously handle off-nominal mission scenarios. These systems will also be capable of mission replanning in the event of unanticipated conditions [59, 60].

Vehicles capable of automatic rendezvous and docking with cooperative and uncooperative target spacecraft will be developed and will be capable of satellite servicing, inspection, retrieval and repair [61, 62].

Wherever navigation system developments lead, one conclusion is **certain**: the continuing and increasing human presence in space, whether through robotic or manned missions, is inevitable. It is our destiny to broaden and **deepen** our understanding of our planet and our solar system, and to apply this knowledge for improving our quality of life on earth. It is also our destiny to build upon our Viking, Voyager, Mariner and Apollo experiences to eventually explore and colonize other planets, other bodies and other solar systems.

ACKNOWLEDGEMENTS

The authors would like to thank Moises Montez of the NASA Johnson Space Center for his assistance in obtaining referenced material and for discussions on Apollo and Shuttle navigation systems. A portion of the research described in this paper was carried out by the C.S. Draper Laboratory (formerly The Massachusetts Institute of Technology Instrumentation Laboratory), and the Jet Propulsion Laboratory, California Institute of Technology under contract with the National Aeronautics and Space Administration.

REFERENCES

1. O'Neil, W. J., et al., Mariner 9 Navigation, Jet Propulsion Laboratory Technical Report 32-1586, Pasadena, CA, Nov. 13, 1973.
2. Wong, S. K., and Lubeley, A. J., "orbit Determination Strategy and Results for the Pioneer 10 Jupiter Mission," AIAA Mechanics and Control of Flight Conference, Anaheim, CA, Aug. 1974.
3. Frauenholz, R. B., and Brady, W. F., "Maneuver Sequence Design for the Post-Jupiter Leg of the Pioneer Saturn Mission," Journal of Spacecraft and Rockets, Vol. 14, July 1977, pp. 395-400.
4. Christensen, C. S., and Reinbold, S. J., "Navigation of the Mariner 10 Spacecraft to Venus and Mercury," Journal of Spacecraft and Rockets, Vol. 12, May 1975, pp. 280-286.
5. O'Neil, W. J., et al., Viking Navigation, Jet Propulsion Laboratory Publication 78-38, Pasadena, CA, Nov. 15, 1979.
6. Wong, S. K., and Guerrero, H. M., "The Strategy and Technique in Determining the Orbits of the Pioneer Venus Multiprobe Bus and Probes," AAS Paper 79-181, AAS/AIAA Astrodynamics Conference, Provincetown, MA, June 1979.
7. Jacobson, R. A., et al., "Orbit Determination Strategy and Results for the Pioneer Venus Orbiter Mission," Advances in the Astronautical Sciences: Astrodynamics 1979, Vol. 40, ed. P. Penzo, et al., Univelt, San Diego, 1980, pp. 251-271.
8. Farquhar, R., Muhonen, D., and Church, L. C., "Trajectories and Orbital Maneuvers for the ISEE-3/ICE Comet Mission," The Journal of the Astronautical Sciences, Vol. 33, July-Sept. 1985, pp. 235-254.
9. Engelhardt, D. B., et al., "Determination and Prediction of Magellan's Orbit," Advances in the Astronautical Sciences: Spaceflight Mechanics 1991, Vol. 75, Pt. II, ed. J. K. Soldner, et al., Univelt, San Diego, 1991, pp. 1143-1160.

10. Cook, R. A., and Lyons, D. T., "Magellan Aerobraking Periapse Corridor Design," Advances in the Astronautical Sciences: Spaceflight Mechanics 1992, Vol. 79, ed. R. Diehl, et al., Univelt, San Diego, 1992., pp. 989-1006.
11. Pollmeier, V. M., and Kallemeyn, P. H., "Galileo Orbit Determination from Launch Through the First Earth Flyby," Proceedings of the 47th Annual Meeting of the Institute of Navigation, Williamsburg, VA, June 1991, pp. 9-16.
12. Kallemeyn, P. H., et al., "Galileo orbit Determination for the Gaspra Asteroid Encounter," Proceedings of the AIAA/AAS Astrodynamics Conference, Hilton Head, SC, Aug. 1992, pp. 370-380.
13. McElrath, T., et al., "Ulysses Navigation at Jupiter Encounter," AIAA Paper 92-4524, AIAA/AAS Astrodynamics Conference, Hilton Head, SC, Aug. 1992.
14. Melbourne, W. G., "Navigation Between the Planets," Scientific American, Vol. 234, June 1976, pp. 58-74.
15. Renzetti, N. A., et al., The Deep Space Network - An Instrument for Radio Navigation of Deep Space Probes, Jet propulsion Laboratory Publication 82-102, Pasadena, CA, Dec. 15, 1982.
16. Jordan, J. F., and Wood, L. J., "Navigation, Space Mission," Encyclopedia of Physical Science and Technology, Vol. 8, Academic Press, 1987, pp. 744-767.
17. Moyer, T. D., Mathematical Formulation of the Double-Precision Orbit Determination Program (DPODP), Jet Propulsion Laboratory Technical Report 32-1527, Pasadena, CA, May 15, 1971.
18. Ekelund, J. E., "The JPL Orbit Determination Software System," in Advances in the Astronautical Sciences: Astrodynamics 1979, Vol. 40, Part 1, ed. P. Penzo, et al., Univelt, San Diego, 1980, pp. 79-88.
19. Hamilton, T. W., and Melbourne, W. G., "Information Content of a Single Pass of Doppler Data from a Distant Spacecraft," in The Deep Space Network, Space Programs Summary 37-39, Vol. HI, Jet Propulsion Laboratory, Pasadena, CA, May 31, 1966, pp. 18-23,
20. Melbourne, W. G., and Curkendall, D. W., "Radio Metric Direction Finding: A New Approach to Deep Space Navigation," AAS/AIAA Astrodynamics Conference, Jackson, WY, Sept. 1977.
21. Campbell, J. K., Synnott, S. P., and Bierman, G. J., "Voyager Orbit Determination at Jupiter," IEEE Transactions on Automatic Control, Vol. AC-28, March 1983, pp. 256-268.
22. Taylor, T. H., et al., "Performance of Difference Range Data Types in Voyager Navigation," Journal of Guidance, Control, and Dynamics, Vol. 7, May-June 1984, pp. 301-306.
23. Jacobson, R. A., Campbell, J. K., and Synnott, S. P., "Satellite Ephemerides for Voyager Saturn Encounter," AIAA Paper 82-1472, AIAA/AAS Astrodynamics Conference, San Diego, CA, August 1982.
24. Campbell, J. K., et al., "Voyager I and Voyager 11 Saturn Encounter Orbit Determination," Paper 82-0419, AIAA 20th Aerospace Sciences Meeting, Orlando, FL, Jan. 1982.
25. Jacobson, R. A., and Standish, E. M., "Satellite Ephemerides for the Voyager Uranus Encounter," AIAA Paper 84-2024, AIAA/AAS Astrodynamics Conf., Seattle, WA, Aug. 1984.
26. Jacobson, R. A., "Satellite Ephemerides for the Voyager Neptune Encounter," Advances in the Astronautical Sciences: Astrodynamics 1987, Vol. 65, Pt. I, ed. J. Soldner, et al., Univelt, San Diego, 1988, pp. 657-680.

27. Gray, D. L., et al., "Voyager 2 Uranus Navigation Results," Proceedings of the AIAA/AAS Astrodynamics Conference, Williamsburg, VA, Aug. 1986, pp. 144-151.
28. Taylor, T. H., et al., "Orbit Determination for the Voyager II Uranus Encounter," Proceedings of the AIAA/AAS Astrodynamics Conference, Williamsburg, VA, Aug. 1986, pp. 178-191.
29. Synnott, S. P., et al., "Interplanetary Optical Navigation: Voyager Uranus Encounter," Proceedings of the AIAA/AAS Astrodynamics Conference, Williamsburg, VA, Aug. 1986, pp. 192-206.
30. Gray, D. L., et al., "Voyager 2 Neptune Navigation Results," Proceeding of the AIAA/AAS Astrodynamics Conference, Portland, OR, Aug. 1990, pp. 108-117.
31. Lewis, G. D., et al., "Voyager 2 Orbit Determination at Neptune," The Journal of the Astronautical Sciences, Vol. 40, July-Sept. 1992, pp. 369-406.
32. Roth, D. C., et al., "Performance of Three-Way Data Types during Voyager's Encounter with Neptune," Proceedings of the AIAA/AAS Astrodynamics Conference, Portland, OR, Aug. 1990, pp. 129-134.
33. Riedel, J. E., et al., "Optical Navigation during the Voyager Neptune Encounter," Proceedings of the AIAA/AAS Astrodynamics Conference, Portland, OR, Aug. 1990, pp. 118-128.
34. Smith, G. H., *Overview of Aerospace Vehicle Computer Applications*, AGARD Computers in the Guidance and Control of Aerospace Vehicles, February, 1972. ⁶
35. *MIT's Role in Project Apollo, Final Report on Contracts NAS 9-153 and NAS 9-4065, Volume I through 5*, M.I.T., Charles Stark Draper Laboratory, Cambridge, MA, October 1971 through August 1972. ⁵
36. Battin, R. H., *Space Guidance Evolution - A Personal Narrative*, Journal of Guidance, Control and Dynamics, March - April 1982. ⁶
37. Brown, R. G., *Integrated Navigation Systems and Kalman Filtering: A Perspective*, Institute of Navigation Journal, Vol. 19, No. 4.
38. Battin, R. H., Article in the New York Times on Eve of Apollo 8, 1965, *In complete*
39. Sears, N. E., *Lunar Mission Navigation Performance of the Apollo Spacecraft Guidance and Navigation Systems*, MIT Charles S. Draper Laboratory, Cambridge, MA, September 1970.
40. Savely, R.T., B.F. Cockrell, S. Pines, *Apollo Experience Report: On-Board Navigation and Alignment Software*, NASA Manned Space Flight Center Internal Note No. 70-FM-171, November 1970.
41. Cockrell, B. F., *Review of Apollo Navigation, Mission Summary and Ground Navigation*, Presentation at Charles S. Draper Laboratory, Lunar/Mars Exploration Navigation Working Group Meeting. *Done?*
42. NASA MSC Internal Note No. 69-FM-209, *Apollo 11 Lunar Trajectory Notes*, July 1969.
43. Schiesser, E., *Navigation for the Apollo 12 Lunar Landing*, Institute of Navigation Proceedings, 1970.
44. Hoag, David G., *The History of Apollo On-Board Guidance, Navigation, and Control*, Charles S. Draper Laboratory, Cambridge, MA, September 1976.
45. Copps, S. L. and J. A. Saponaro, *Operations and Functions of the Apollo Guidance Computer During Rendezvous*, MIT Instrumentation Laboratory, Cambridge, MA, November 1969.
46. Schiesser, E., *Navigation for the Apollo 12 Lunar Landing*, Institute of Navigation Proceedings, 1970.
47. Battin, R. H. and G. E. Levine, *Application of Kalman Filtering Techniques to the Apollo*

- Program, MIT Instrumentation Laboratory, Cambridge, MA, April 1969.
48. Muller, E. S. and P. M. Kachmar, *The Apollo Rendezvous Navigation Filter Theory, Description and Performance, Volume 1*, MIT Charles S. Draper Laboratory, June 1970.
 49. Sears, Norman E. (Editor), *Primary G&N System Lunar Orbit Operations, Volume 1 and 2*, MIT Instrumentation Laboratory, Cambridge, MA, April 1964.
 50. Baker, D. S., N. E. Sears and R. L. White, *Lunar Orbit Navigation with Various Random and Systematic Errors*, MIT Instrumentation Laboratory, Cambridge, MA, July 1966.
 51. Baker, D. S., N. E. Sears, J. B. Suomals, and R.L. White, *Lunar Orbit determination by Star Occultation and MSFN Tracking*, MIT Instrumentation Laboratory, Cambridge, MA, September 1963.
 52. Schmidt, Thomas G., *Ascent and Entry Navigation of the Shuttle*, AAS 91-150
 53. Savely, R. T., B. F. Cockrell, *Shuttle Navigation Overview*, AIAA, A82-39000 Guidance and Control Conference, San Diego, CA, August 1982.
 54. Kachmar, P., W. Chu, and R. J. Polutchko, *Use of a Laser Navigation Sensor for Automatic Rendezvous*, Institute of Navigation Journal, Volume 39, No, 1, Spring 1992
 55. Kachmar, P. W., Chu, and P. J. Neirinckx, "U. S. Space Shuttle: Integrated GPS Navigation Capability" Institute of Navigation GPS-93 Conference, Salt Lake City, Utah, September 1993
 56. Brown, A. K., and J. W. Larrakas, *An Overview of Space-Based Radionavigation Systems*, IEEE, November 1988
 57. Nunjal, P., W. Feess, and M. Ananda, *A Review of Spaceborne Application of GPS*, Institute Of Navigation Journal Paper, September 1992
 58. Brand, T. J., and S. W. Shepperd, "Candidate Mars Local Navigation Infrastructures", AAS/AIAA Astrodynamics Specialist Conference, Durango, Colorado, August 1991.
 59. Gafney, J.E, Jr., *Navigation in Space, The future, and Artificial Intelligence*, Institute of Navigation Journal, Winter 1973.
 60. Mayer, G., *Radio Interferometric Techniques and Their Impact on Aeronautical and Space Navigation jibe Future*, Journal Article, January 1988. *incomplete*
 61. Brewing, C. C., and K. W. Braden, *Application of Advanced Guidance and Navigation Systems to Flight Control of Aircraft and Future Space Systems*, SPIE, Vol. 1694, 1992
 62. Kachmar, P. M., and W. Jackson, "Automatic Rendezvous and Capture System Development in a Manned Environment" NASA Automated Rendezvous and Capture Review Conference, Williamsburg, VA, November 1991.

Figures:

- 1.0 Planetary Robotic Missions - Voyager
- 2.0 Apollo Manned Missions
- 3.0 Deep Space Navigation System
- 4.0 Characteristics of Doppler as a Deep Space Navigation Measurement
- 5.0 Inertial Measurement Unit
- 6.0 Apollo Space Sextant
- 7.0 Simplified Apollo Recursive Navigation Functional Diagram
- 8.0 Apollo Command and Service Module Navigation Sensors
- 9.0 Apollo Lunar Excursion Module Navigation Sensors
- 10. Shuttle Mission Profile
- 11. Shuttle Navigation Sensors